JOURNAL OF QUATERNARY SCIENCE (2009)

Published online in Wiley InterScience
(www.interscience.wiley.com) DOI: 10.1002/jqs.1308

Age assignment of a diatomaceous ooze deposited in the western Amundsen Sea Embayment after the Last Glacial Maximum

CLAUS-DIETER HILLENBRAND,[1]* JAMES A. SMITH,[1] GERHARD KUHN,[2] OLIVER ESPER,[2] RAINER GERSONDE,[2] ROB D. LARTER,[1] BARBARA MAHER,[3] STEVEN G. MORETON,[4] TRACY M. SHIMMIELD[5] and MONIKA KORTE[6]

[1] British Antarctic Survey (BAS), Cambridge, UK
[2] Alfred Wegener Institute for Polar and Marine Research (AWI), Bremerhaven, Germany
[3] Centre for Environmental Magnetism and Palaeomagnetism, Lancaster Environment Centre, Lancaster University, Lancaster, UK
[4] NERC Radiocarbon Facility (Environment), East Kilbride, UK
[5] Scottish Association for Marine Science (SAMS), Dunstaffnage Marine Laboratory, Oban, UK
[6] Helmholtz-Zentrum Potsdam, Deutsches GeoForschungsZentrum (GFZ), Potsdam, Germany

Hillenbrand, C.-D., Smith, J. A., Kuhn, G., Esper, O., Gersonde, R., Larter, R. D., Maher, B., Moreton, S. G., Shimmield, T. M. and Korte, M. Age assignment of a diatomaceous ooze deposited in the western Amundsen Sea Embayment after the Last Glacial Maximum. *J. Quaternary Sci.*, (2009). ISSN 0267-8179.

Received 20 December 2008; Revised 24 April 2009; Accepted 13 May 2009

ABSTRACT: Reliable dating of glaciomarine sediments deposited on the Antarctic shelf since the Last Glacial Maximum (LGM) is challenging because of the rarity of calcareous (micro-) fossils and the recycling of fossil organic matter. Consequently, radiocarbon (^{14}C) ages of the acid-insoluble organic fraction (AIO) of the sediments bear uncertainties that are difficult to quantify. Here we present the results of three different methods to date a sedimentary unit consisting of diatomaceous ooze and diatomaceous mud that was deposited following the last deglaciation at five core sites on the inner shelf in the western Amundsen Sea (West Antarctica). In three cores conventional ^{14}C dating of the AIO in bulk samples yielded age reversals down-core, but at all sites the AIO ^{14}C ages obtained from diatomaceous ooze within the diatom-rich unit yielded similar uncorrected ^{14}C ages between 13 517 ± 56 and 11 543 ± 47 years before present (a BP). Correction of these ages by subtracting the core-top ages, which probably reflect present-day deposition (as indicated by ^{210}Pb dating of the sediment surface at one core site), yielded ages between ca. 10 500 and 8400 cal. a BP. Correction of the AIO ages of the diatomaceous ooze by only subtracting the marine reservoir effect (MRE) of 1300 a indicated deposition of the diatom-rich sediments between 14 100 and 11 900 cal. a BP. Most of these ages are consistent with age constraints between 13.0 and 8.0 ka for the diatom-rich unit, which we obtained by correlating the relative palaeomagnetic intensity (RPI) records of three of the sediment cores with global and regional reference curves. As a third dating technique we applied conventional radiocarbon dating of the AIO included in acid-cleaned diatom hard parts extracted from the diatomaceous ooze. This method yielded uncorrected ^{14}C ages of only 5111 ± 38 and 5106 ± 38 a BP, respectively. We reject these young ages, because they are likely to be overprinted by the adsorption of modern atmospheric carbon dioxide onto the surfaces of the diatom hard parts prior to sample graphitisation and combustion for ^{14}C dating. The deposition of the diatom-rich unit in the western Amundsen Sea suggests deglaciation of the inner shelf before ca. 13 ka BP. The deposition of diatomaceous oozes elsewhere on the Antarctic shelf around the same time, however, seems to be coincidental rather than directly related. Copyright © 2009 John Wiley & Sons, Ltd.

KEYWORDS: Antarctica; Holocene; radiocarbon; relative palaeomagnetic intensity; sediment chronology.

Introduction

Reliable dating of Southern Ocean sediments deposited south of the Antarctic Polar Front (APF) during the last climatic cycle is a major challenge for Quaternary chronology (e.g. Andrews *et al.*, 1999; Heroy and Anderson, 2007). The dating problems arise mainly from the lack of calcareous (micro-)fossils in most glaciomarine sediments deposited in the seasonal sea ice zone. In Southern Ocean sediments calcareous material usually provides the most reliable accelerator mass spectrometry (AMS) ^{14}C ages, at least for the time since the Last Glacial Maximum (LGM) (e.g. Anderson *et al.*, 2002; Bianchi and Gersonde, 2004; Bentley *et al.*, 2005; Domack *et al.*, 2005; Heroy and

* Correspondence to: C.-D. Hillenbrand, British Antarctic Survey (BAS), High Cross, Madingley Road, Cambridge CB3 0ET, UK.
E-mail: hilc@bas.ac.uk

Anderson, 2005, 2007; Rosenheim *et al.*, 2008), and allows the application of other dating techniques, such as amino acid racemisation (e.g. Forsberg *et al.*, 2003), electron spin resonance dating (e.g. Takada *et al.*, 2003; Theissen *et al.*, 2003) or U-series/U–Th dating methods (e.g. Goldstein *et al.*, 2001). Glacial and glaciomarine sediments deposited on the Antarctic continental margin since the LGM at ca. 23–19 cal. ka BP are often barren of biogenic carbonate. Chronologies for these sequences are commonly established by AMS ^{14}C dating of the acid-insoluble organic fraction (AIO) from bulk sediment samples. The AIO is mainly derived from diatomaceous organic matter, and its dating has been assumed to provide reasonable age models for sediment cores recovered from the Antarctic shelf (e.g. Licht *et al.*, 1996, 1998; Andrews *et al.*, 1999; Domack *et al.*, 1999a, 2001; Licht and Andrews, 2002; Ó Cofaigh *et al.*, 2005; Pudsey *et al.*, 2006).

However, AMS ^{14}C dates of the AIO from surface seafloor sediments around Antarctica frequently yield ages of several thousand years (e.g. Andrews *et al.*, 1999; Pudsey *et al.*, 2006). These old surface ages can partly be attributed to the marine reservoir effect (MRE). The MRE south of the APF is in the range 750–1300 ^{14}C a, two to three times larger than the global MRE of ca. 400 a (Gordon and Harkness, 1992; Berkman and Forman, 1996; Domack *et al.*, 1999a, 2005; Reimer and Reimer, 2001). Another major factor causing the unusually 'old' AIO ages of seabed sediments in the Southern Ocean is the flux of ^{14}C-depleted particulate organic matter. The most significant contribution is fossil carbon derived from glacial erosion on the Antarctic continent, but the reworking of unconsolidated sediments also plays a role. This fossil organic material is mixed into the marine sediments in unknown amounts. Antarctic shelf sediments are particularly susceptible to this kind of contamination, because their low bulk organic carbon content makes the AMS ^{14}C ages very sensitive to even small amounts of fossil carbon. As a consequence, the AIO ages of surface sediments vary by up to several thousand years between different regions of the Antarctic shelf and between different core sites in the same region, for example between ca. 1500 and 7500 ^{14}C a BP on the western Ross Sea shelf (DeMaster *et al.*, 1996; Andrews *et al.*, 1999) and between ca. 5500 and 17 300 ^{14}C a BP on the Larsen Shelf, east of the Antarctic Peninsula (Pudsey *et al.*, 2006). Furthermore, down-core AIO ages often produce inconsistent age–depth profiles including age reversals (e.g. Licht and Andrews, 2002; Mosola and Anderson, 2006).

The occurrence of old surface ages combined with the potential error in down-core AIO ages complicates the reliability of ^{14}C-based age models for post-LGM sedimentary sequences south of the APF. Usually, down-core AIO ages are corrected by subtracting the core-top age (e.g. Andrews *et al.*, 1999; Domack *et al.*, 1999a; Mosola and Anderson, 2006; Pudsey *et al.*, 2006). This approach assumes that (i) the core top represents modern sedimentation, and (ii) the contribution of reworked fossil carbon from the hinterland remained constant through time. The first assumption can be validated by deploying coring devices that are capable of recovering undisturbed sediment samples from the modern seabed surface (e.g. box and multiple corers), paired ^{14}C dating of the AIO and calcareous (micro-)organisms (if present) and application of ^{210}Pb dating in addition to AIO ^{14}C dating (e.g. Harden *et al.*, 1992; Andrews *et al.*, 1999; Domack *et al.*, 2001, 2005; Pudsey *et al.*, 2006). The validity of the second assumption might be tested by paired ^{14}C down-core dating of both AIO and calcareous material (e.g. Licht *et al.*, 1998; Domack *et al.*, 2001; Licht and Andrews, 2002; Rosenheim *et al.*, 2008). However, this method is inapplicable in most cases due to the general absence of calcareous (micro-)fossils in Antarctic shelf sediments (e.g. Domack *et al.*, 1999a; Mosola and Anderson, 2006; Pudsey *et al.*, 2006).

Indeed, there is evidence that the degree of contamination with ^{14}C-depleted organic matter is negatively correlated with the distance of a core site from the ice sheet grounding line, which represents the source of the contamination (e.g. Domack, 1992). This distance, however, was reduced during the past, when the Antarctic ice sheets had advanced across the shelf (e.g. Anderson *et al.*, 2002). Therefore, AIO-based ^{14}C chronologies for the last deglaciation of the Antarctic shelf bear some uncertainty (e.g. Pudsey *et al.*, 2006; Heroy and Anderson, 2007; Rosenheim *et al.*, 2008). As a consequence, it is still unclear if the deglaciation of the Antarctic shelf after the LGM occurred synchronously (Siegert *et al.*, 2008) or was time transgressive (Anderson *et al.*, 2002).

Recent progress towards more reliable methods for dating of organic matter in Antarctic marine sediments has been made by compound-specific radiocarbon dating (Ohkouchi *et al.*, 2003; Ingalls *et al.*, 2004; Ohkouchi and Eglinton, 2006, 2008) and stepped-combustion AMS ^{14}C dating (Rosenheim *et al.*, 2008). Most of these methods, however, are laborious, time consuming, technologically challenging and still under development (e.g. Ingalls *et al.*, 2004; Ohkouchi and Eglinton, 2008; Rosenheim *et al.*, 2008). Alternative techniques for establishing more reliable age models for Holocene sedimentary sequences recovered south of the APF use the palaeomagnetic intensity record of the sediment cores (Brachfeld *et al.*, 2003; Willmott *et al.*, 2006) or ^{226}Ra activities in marine barite (Van Beek *et al.*, 2002). The latter method, however, is extremely challenging and expensive because it requires measurement of gamma activity in high-efficiency, low-background, well-type detectors in specialised underground laboratories (Van Beek *et al.*, 2002).

During cruises JR141 with RRS *James Clark Ross* and ANT-XXIII/4 with RV *Polarstern* in 2006, 55 vibro- and gravity cores were deployed on the West Antarctic shelf in the Amundsen Sea to reconstruct the size of the LGM ice sheet and its subsequent retreat pattern (Fig. 1; Gohl, 2007; Larter *et al.*, 2007). Five sediment cores that were collected from the inner shelf in the western Amundsen Sea Embayment (ASE) recovered a prominent subsurface lithological unit consisting of diatomaceous ooze and diatomaceous mud of apparently post-LGM age. The relatively low content of terrigenous detritus in the diatomaceous ooze of this unit offered the rare possibility to obtain AMS ^{14}C dates on AIO that is largely unaffected by contamination from terrigenous fossil carbon (e.g. DeMaster *et al.*, 1996; Andrews *et al.*, 1999). In this paper, we present and compare the results of three different dating techniques applied to constrain the age of the diatom-rich unit: (i) conventional AMS ^{14}C dating of the bulk AIO in all of the cores; (ii) AMS ^{14}C dating of the AIO enclosed in biosiliceous hard parts extracted from the diatomaceous ooze in one of the cores; and (iii) dating of three of the cores by using their relative palaeomagnetic intensity (RPI) records.

Materials and methods

Sediment cores

Vibro-cores VC424 and VC425 were recovered north of the Getz Ice Shelf between Wright Island and Martin Peninsula (Getz 'A' Ice Shelf; Fig. 1, Table 1). Gravity cores PS69/273-2, PS69/274-1 and PS69/275-1 were collected from a deep inner shelf basin north of the Getz Ice Shelf between Carney Island and Wright Island (Getz 'B' Ice Shelf; Fig. 1, Table 1). The inner shelf between Carney Island and Martin Peninsula forms part of a glacial trough that extends in a N to NW direction towards the

DOI: 10.1002/jqs

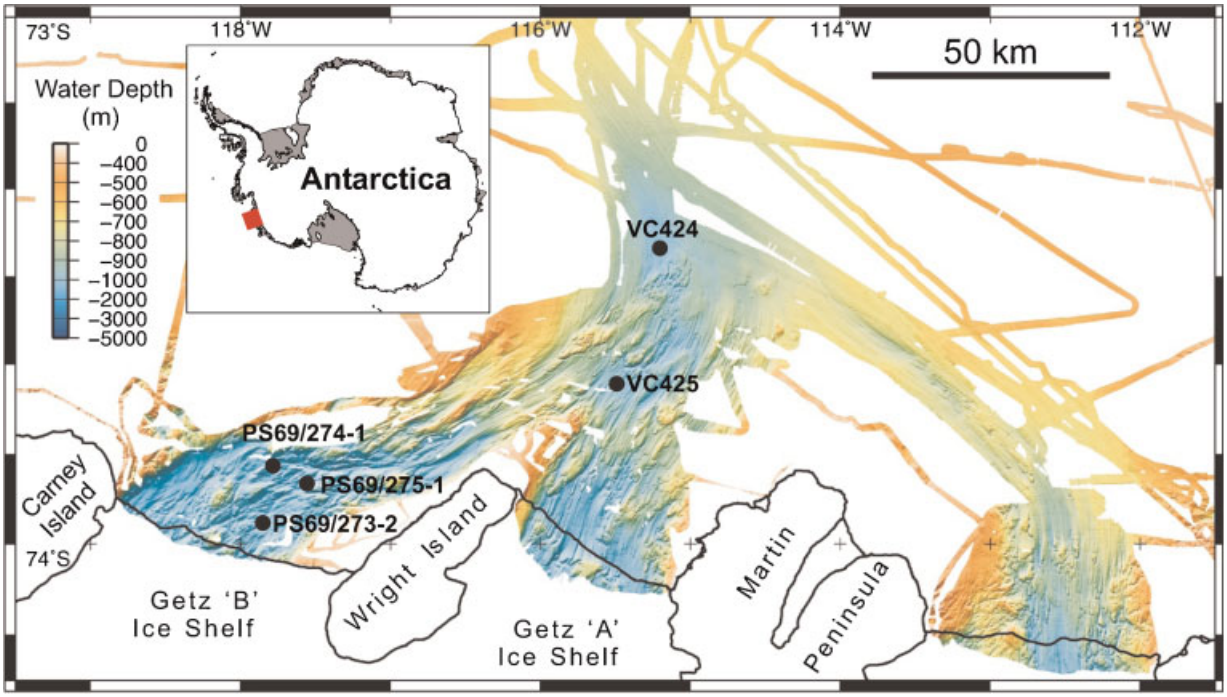

Figure 1 Location of the study area (red rectangle in inset figure) and multi-beam bathymetry map of the western Amundsen Sea Embayment with sites of marine sediment cores and geographical locations mentioned in the text (modified from Larter *et al.*, 2009)

outer shelf (Larter *et al.*, 2007, 2009; Nitsche *et al.*, 2007). In addition to the vibro- and gravity cores, box cores were collected in order to obtain undisturbed sediment surface samples from the seafloor. Box core BC423 was recovered from the same site as vibro-core VC424 and giant box core PS69/275-2 was taken from gravity core site PS69/275-1.

Lithology and structures of the recovered sedimentary sequences were described on the split cores and on X-radiographs. Shear strength (SS) was analysed on all gravity and vibro-cores at intervals from 10 to 20 cm using a hand-held shear vane. Volume-specific magnetic susceptibility (MS; in dimensionless SI units) was measured on split cores at 1 cm intervals (VC425: 2 cm intervals) using a Bartington MS2 susceptibility meter with MS2F sensor. Additionally, volume-specific MS and wet-bulk density (WBD) were analysed at 1 cm intervals on whole cores PS69/273-2, PS69/274-1, PS69/275-1 (outer core diameter 12.5 cm) and VC424 (outer core diameter 8.5 cm) with a GEOTEK multi-sensor core logger (MSCL; fitted with a Bartington MS2 susceptibility meter with a MS2C loop sensor of diameter 14 cm) onboard RV *Polarstern* and at the British Ocean Sediment Core Research Facility (BOSCORF) in Southampton (UK), respectively.

Contents of total organic carbon (TOC) and biogenic opal were measured on discrete sediment samples taken at 10 cm intervals from core PS69/274-1 using a LECO CS-125 carbon determinator and an automated leaching technique (Müller and Schneider, 1993), respectively. The latter method was shown to be reliable in an inter-laboratory comparison (Conley, 1998), but usually gives biogenic opal contents significantly lower than those estimated from the abundance of siliceous microfossils in smear slides (cf. Hillenbrand and Fütterer, 2002; Pudsey, 2002). Sample treatment and preparation of quantitative diatom slides for light microscopy followed the standard procedure developed at the Alfred Wegener Institute for Polar and Marine Research (AWI) (Zielinski and Gersonde, 1997; Gersonde and Zielinski, 2000) and the counting method according to Schrader and Gersonde (1978). Diatom concentrations were calculated from the census data, which will be presented in detail in a separate publication, and are given in valves per gram dry sediment.

Detailed lithological descriptions, photos and X-radiographs of the cores and all data published in this paper are available from the PANGAEA world data centre (http://doi.pangaea.de/) under doi: 10.1594/PANGAEA.715974.

Table 1 Metadata for the sediment cores recovered from the inner shelf in the western Amundsen Sea Embayment

Expedition	Core	Gear	Latitude (S)	Longitude (W)	Water depth (m)	Recovery (cm)	Top and base of diatom-rich unit (cmbsf)
ANT-XXIII/4	PS69/273-2	GC	73° 57.7′	117° 50.6′	1352	329	163–219
ANT-XXIII/4	PS69/274-1	GC	73° 51.4′	117° 46.5′	1452	453	196–238
ANT-XXIII/4	PS69/275-1	GC	73° 53.3′	117° 32.9′	1518	479	191–207
ANT-XXIII/4	PS69/275-2	GBC	73° 53.3′	117° 32.9′	1517	26	—
JR141	BC423	BC	73° 26.8′	115° 11.9′	1073	41	—
JR141	VC424	VC	73° 26.8′	115° 11.9′	1073	537	198–277
JR141	VC425	VC	73° 42.2′	115° 29.2′	1020	508	221–224

GC: gravity core; GBC: giant box core; BC: box core; VC: vibro-core.

DOI: 10.1002/jqs

Determination of excess ^{210}Pb activity

In order to evaluate whether the seafloor surface sediment recovered with box core PS69/275-2 is associated with recent deposition or whether it is condensed, affected by erosion, winnowing or sediment mixing induced by strong bottom currents, down-slope processes or bioturbation (e.g. Domack *et al.*, 1999b, 2005), we determined excess ^{210}Pb activity by analysing total ^{210}Pb and ^{226}Ra on bulk samples from a sub-core (cf. Howe *et al.*, 2004). The measurements were carried out at SAMS in Oban (UK) using gamma spectroscopy. Approximately 10 g of freeze-dried sediment at 1 cm intervals was carefully weighed into a plastic lid, pressed, and sealed for at least 24 days prior to analysis using high-purity germanium detectors (Hp Ge).

AMS ^{14}C dating and calibration of the ^{14}C ages

All samples selected for AMS ^{14}C dating were prepared to graphite at the NERC Radiocarbon Laboratory in East Kilbride (UK). As a pre-treatment the raw samples were digested in 2M HCl at 80°C for 8 h, washed free from mineral acid with deionised water, then dried and homogenised. The total acid-insoluble organic carbon in a known weight of the pre-treated sample was recovered as carbon dioxide (CO_2) by heating with CuO in an evacuated, sealed quartz tube. The gas was converted to graphite by Fe/Zn reduction. After preparation to graphite the samples were passed to the SUERC AMS Facility in East Kilbride (UK). We dated the AIO of bulk sediment samples taken from all of the cores and the AIO in cleaned diatom hard parts. All samples from the diatom-rich sedimentary unit were taken from diatomaceous ooze.

Diatom hard parts comprising frustules, girdle bands, spines and setae were extracted from diatomaceous ooze in core PS69/274-1 at the AWI in Bremerhaven (Germany). Three slices of wet sediment were freeze-dried (dry weight of samples 12–14 g), and organic carbon was removed from the dry sediment by treating the samples with a cold-saturated solution of potassium permanganate for 24 h. The samples were heated to boiling point and a saturated solution of HCl (37%) was added to dissolve carbonate. Afterwards, any residual carbon adhering to the hard parts was removed with concentrated hydrogen peroxide (35%). Half a spoonful of crystal sodium polyphosphate was added to each sample to prevent the particles from aggregating. After cooling, the samples were diluted with water (~10 times the sample volume) and sieved over a 10 μm nylon sieve. We checked after each sieving step whether material from the sieve mesh had contaminated the sample. No such contamination was observed. The sieved residue was dried overnight (dry weight of residues 2–5 g) and stored in glass vials to prevent contamination by inorganic carbon. The TOC content measured on the extracted and cleaned diatom hard parts was 0.2 wt% (Table 2), suggesting that organic material included within the opal of the diatoms was not significantly affected by the oxidisation procedure.

We give the radiocarbon ages as conventional, i.e. uncorrected, ^{14}C years before present (BP; relative to AD 1950) and calibrated years BP (cal. a BP). We assume that the offset between the modern MRE on the Antarctic shelf (ca. 1300 a; e.g. Berkman and Forman, 1996) and the uncorrected ^{14}C ages of the surface sediment samples taken from box cores BC423 and PS69/275-2 (Table 2) is caused by local contamination with fossil organic matter that is supplied with terrigenous detritus. We refer to this age difference as 'local contamination offset' (LCO). Before calibrating the ^{14}C dates, we subtracted the LCO obtained for site PS69/275-2 from the conventional ^{14}C down-core ages of cores PS69/273-2, PS69/274-1 and PS69/275-1, and the LCO obtained for site BC423 from the conventional ^{14}C down-core ages in cores VC424 and VC425 (Table 2).

In the western and central Ross Sea, DeMaster *et al.* (1996) and Andrews *et al.* (1999) had obtained AIO ^{14}C ages from 49 seabed sediment surface samples. The youngest uncorrected AIO ages reported in the two studies range from 1500 to 2600 ^{14}C a, which is just ~1–2 times the MRE. These ages were obtained from samples with relatively high TOC contents (1.2–2.1 wt%) and maximum biogenic opal contents (37–53 wt%), for example from surface sediments in Granite Harbor on the inner shelf (for location see Fig. 7). DeMaster *et al.* (1996) concluded that contents of TOC and opal in Antarctic shelf sediments can be used as proxies for marine plankton productivity. Consequently, Andrews *et al.* (1999) suggested that AIO ^{14}C ages of shelf sediments resulting from high productivity, such as diatomaceous oozes, provide more reliable dates than other sediments. Based on these findings, we applied an alternative correction to the conventional ^{14}C ages obtained from the diatomaceous ooze in the cores from the western ASE by only subtracting the MRE, thereby assuming that the AIO in those samples is unaffected by contamination with fossil carbon (Table 2).

We calibrated all ^{14}C ages with the CALIB Radiocarbon Calibration Program version 5.0.2html (http://calib.qub.ac.uk/calib/; Stuiver *et al.*, 2005) using the Marine04 calibration dataset (Hughen *et al.*, 2004) and assuming a regional marine offset (ΔR) of 900 ± 100 a from the global MRE in accordance with the ΔR used in previous studies from the ASE (e.g. Anderson *et al.*, 2002) and the ΔR given in the marine reservoir correction database (http://intcal.qub.ac.uk/marine/; Reimer and Reimer, 2001).

Measurements of magnetic parameters and modelling of RPI

The orientated samples for magnetic measurements were taken at 7 cm intervals from the postglacial sediments in cores VC424, PS69/274-1 and PS69/275-1 using cubic plastic boxes ($2 \times 2 \times 2$ cm). The discrete samples were analysed at the Centre for Environmental Magnetism and Palaeomagnetism in Lancaster (UK) with a JR6A spinner magnetometer (AGICO), an alternating-field (AF) shielded demagnetiser with tumbling mechanism (Molspin Ltd) and a Bartington MS2 susceptibility meter using an MS2B sensor. We analysed inclination, declination, natural remanent magnetisation (NRM) and anhysteretic remanent magnetisation (ARM), subsequently AF-demagnetised at both 0 mT and 20 mT, and the low-frequency volume-specific MS (κ). The vibro- and gravity cores were orientated only with respect to the vertical axis, and therefore we do not present and discuss results referring to the declination. Following other palaeomagnetic studies carried out on the West Antarctic continental margin (Macri *et al.*, 2006; Willmott *et al.*, 2006) we calculated the RPI as the ratio between the NRM intensity AF-demagnetised at 20 mT (NRM_{20mT}) and the ARM intensity AF-demagnetised at 20 mT (ARM_{20mT}). As a proxy for magnetic grain size, we calculated the ratio between ARM and κ (e.g. Maher, 1988; Sagnotti *et al.*, 2001; Brachfeld *et al.*, 2003; Macri *et al.*, 2006). We calculated the mass-specific MS (χlf) for the discrete samples from κ by using the WBD data measured with the MSCL. We used the palaeomagnetic intensity curves published by Yang *et al.* (2000) and Knudsen *et al.* (2008) as global reference curves,

DOI: 10.1002/jqs

Table 2 Conventional, corrected and calibrated AMS ^{14}C ages analysed on the acid-insoluble fraction of the organic matter (AIO) for all studied cores. Percentages of total organic carbon (TOC), δ^{13}C ratios of the TOC, local contamination offset (LCO), and ΔR are also given (δ^{13}C ratios given in italics are estimated). Note: AMS ^{14}C dates of surface sediment samples and a sample with an uncorrected age >26 ^{14}C ka BP could not be calibrated

Core	Sample depth (cmbsf)	Lithology	Lithological unit	Laboratory code	Conventional ^{14}C age (^{14}C a BP)	TOC (wt%)	δ^{13}C (‰ VPDB)	LCO (a)	LCO corr. age (corr. ^{14}C a BP)	ΔR (a)	Calibrated age CALIB 5.0.2 (cal. a BP)
PS69/273-2	191.5–192.5	Diatomaceous ooze	II	SUERC-13342	11 945 ± 38	0.9	−27.9	2650	9 295	900 ± 100	8 988
PS69/273-2	191.5–192.5	Diatomaceous ooze	II	SUERC-13342	11 945 ± 38	0.9	−27.9	0	11 945	900 ± 100	12 659
PS69/274-1	59.5–60.5	Mud	I	SUERC-14428	7 740 ± 39	0.4	−26.1	2650	5 090	900 ± 100	4 272
PS69/274-1	139.5–140.5	Mud	I	SUERC-14429	14 199 ± 61	0.2	*−25.0*	2650	11 549	900 ± 100	11 968
PS69/274-1	176.5–177.5	Mud	I	SUERC-21448	14 821 ± 64	0.5	−26.0	2650	12 171	900 ± 100	12 862
PS69/274-1	209.5–210.5	Diatomaceous ooze	II	SUERC-15252	12 034 ± 69	0.8	−29.7	2650	9 384	900 ± 100	9 112
PS69/274-1	209.5–210.5	Diatomaceous ooze	II	SUERC-15252	12 034 ± 69	0.8	−29.7	0	12 034	900 ± 100	12 739
PS69/274-1	231.5–232.5	Diatomaceous ooze	II	SUERC-11798	11 967 ± 49	0.6	*−25.0*	2650	9 317	900 ± 100	9 021
PS69/274-1	231.5–232.5	Diatomaceous ooze	II	SUERC-11798	11 967 ± 49	0.6	*−25.0*	0	11 967	900 ± 100	12 681
PS69/274-1	221–224_a	Extracted diatoms	II	SUERC-16511	5 111 ± 38	0.2	−27.5	2650	2 461	900 ± 100	1 113
PS69/274-1	221–224_a	Extracted diatoms	II	SUERC-16511	5 111 ± 38	0.2	−27.5	0	5 111	900 ± 100	4 299
PS69/274-1	221–224_b	Extracted diatoms	II	SUERC-16512	5 106 ± 38	0.2	−27.4	2650	2 456	900 ± 100	1 108
PS69/274-1	221–224_b	Extracted diatoms	II	SUERC-16512	5 106 ± 38	0.2	−27.4	0	5 106	900 ± 100	4 293
PS69/274-1	311.5–312.5	Mud	IIIa	SUERC-21449	24 416 ± 198	0.2	−25.6	2650	21 766	900 ± 100	24 543
PS69/275-2	0–1	Mud	I	SUERC-13341	3 950 ± 35	0.6	−26.5	2650	1 300	900 ± 100	n.a.
PS69/275-1	52.5–53.5	Mud	I	SUERC-21450	8 795 ± 42	0.4	−25.9	2650	6 145	900 ± 100	5 613
PS69/275-1	107.5–108.5	Mud	I	SUERC-14427	13 154 ± 56	0.3	−25.4	2650	10 504	900 ± 100	10 454
PS69/275-1	203.5–204.5	Diatomaceous ooze	II	SUERC-11799	11 543 ± 47	0.6	*−25.0*	2650	8 893	900 ± 100	8 467
PS69/275-1	203.5–204.5	Diatomaceous ooze	II	SUERC-11799	11 543 ± 47	0.6	*−25.0*	0	11 543	900 ± 100	11 956
PS69/275-1	228–229	Mud	IIIa	SUERC-21451	15 703 ± 69	0.4	−25.4	2650	13 053	900 ± 100	13 598
PS69/275-1	429.5–430.5	Mud	IV	SUERC-21452	28 020 ± 311	0.1	−25.8	2650	25 370	900 ± 100	n.a.
BC423	0–1	Mud	I	SUERC-13338	4 289 ± 35	0.8	−26.7	2989	1 300	900 ± 100	n.a.
VC424	83.5–84.5	Mud	I	SUERC-14426	8 108 ± 40	0.9	−26.7	2989	5 119	900 ± 100	4 310
VC424	204–205	Diatomaceous ooze	II	SUERC-21453	12 183 ± 51	0.9	−28.0	2989	9 194	900 ± 100	8 838
VC424	204–205	Diatomaceous ooze	II	SUERC-21453	12 183 ± 51	0.9	−28.0	0	12 183	900 ± 100	12 870
VC424	265.5–266.5	Diatomaceous ooze	II	SUERC-11800	11 803 ± 48	0.8	*−25.0*	2989	8 814	900 ± 100	8 381
VC424	265.5–266.5	Diatomaceous ooze	II	SUERC-11800	11 803 ± 48	0.8	*−25.0*	0	11 803	900 ± 100	12 455
VC424	275.5–276.5	Diatomaceous ooze	II	SUERC-21456	13 517 ± 56	0.9	−26.5	2989	10 528	900 ± 100	10 481
VC424	275.5–276.5	Diatomaceous ooze	II	SUERC-21456	13 517 ± 56	0.9	−26.5	0	13 517	900 ± 100	14 103
VC425	220.5–221.5	Diatomaceous ooze	II	SUERC-14423	12 868 ± 54	0.9	−26.8	2989	9 879	900 ± 100	9 691
VC425	220.5–221.5	Diatomaceous ooze	II	SUERC-14423	12 868 ± 54	0.9	−26.8	0	12 868	900 ± 100	13 420

DOI: 10.1002/jqs

and an RPI curve from the shelf west of the Antarctic Peninsula (Willmott *et al.*, 2006) as a regional reference curve. Willmott *et al.* (2006) established the chronology for the RPI curve from the Antarctic Peninsula shelf by correlation with a global RPI stack (Yang *et al.*, 2000; Laj *et al.*, 2002) and a well-dated high-resolution RPI curve from North America (St-Onge *et al.*, 2003).

Sedimentary sequences and chronological data

Lithology and sedimentary structures

The uppermost lithological unit (Unit I) at the five core sites consists of 163–221 cm thick, dark brownish-grey to dark olive-grey muds and silty clays, which contain diatoms ($\leq 43 \times 10^6$ valves g^{-1}), but are dominated by terrigenous components. In core PS69/274-1 the biogenic opal content of Unit I is 2–7 wt%. The TOC content reaches 0.9 wt% at the core top and varies from 0.2 to 0.7 wt% in the rest of Unit I (Fig. 2). Unit I is moderately to strongly bioturbated with subordinate lamination and stratification. In Unit I of cores PS69/273-2, PS69/274-1 and PS69/275-1, the MS ranges from 50 to 200×10^{-5} SI units, and the SS is usually $\leq$6 kPa except for the middle part of Unit I, where SS increases up to 10 kPa (Fig. 2). In cores VC424 and VC425, the MS of Unit I varies only between 25 and 90×10^{-5} SI units, and SS ranges from 1 to 4 kPa (Fig. 2). We interpret Unit I to be a glaciomarine sequence, deposited in a seasonally open-water environment similar to the present day.

Unit I is underlain by an olive-grey unit consisting of diatomaceous ooze and diatomaceous mud (Unit II), which exhibits a bioturbated top and a sharp base. The thickness of Unit II varies from ~3 to 79 cm between the core sites (Table 1). The sedimentary structures within Unit II comprise strong bioturbation as well as parallel to lenticular lamination and stratification. Unit II in cores PS69/273-2, PS69/274-1, PS69/275-1 and VC425 consists mainly of diatomaceous ooze, while Unit II in core VC424 comprises eight, 2–7 cm thick diatomaceous ooze layers alternating with nine, 2–16 cm thick diatomaceous mud layers. In core PS69/274-1 the diatom concentration in the diatomaceous ooze of Unit II reaches 234×10^6 valves g^{-1}, biogenic opal content is 33–38 wt% and TOC content is 0.6–0.9 wt% (Fig. 2). The diatom abundance and biogenic opal content in the diatomaceous ooze of Unit II are comparable with those of modern surface sediments from the 'opal belt' in the pelagic Southern Ocean (e.g. Zielinski and Gersonde, 1997; Geibert *et al.*, 2005). In all cores, Unit II exhibits extremely low MS values, reflecting the low content of terrigenous particles. The down-core MS profiles of cores PS69/273-2, PS69/274-1, PS69/275-1, VC424 and VC425 can be used for inter-core correlation of lithological Units I and II (Fig. 3). MS variability within Unit II, e.g. in core PS69/273-2 and particularly in core VC424 (Figs 2, 3), is probably related to changes in biogenic opal content.

The diatomaceous ooze in Unit II of cores PS69/273-2, PS69/274-1, PS69/275-1 and VC425 is characterised by the extraordinarily well-preserved diatom species *Corethron pennatum* (= *C. criophilum*; Crawford *et al.*, 1998). The *C. pennatum* frustules dominate in sedimentological smear slides, but diatom counts on slides prepared for quantitative species analysis reveal that their abundance within Unit II varies from 4% to 65% (e.g. in core PS69/274-1). Other significant (>2%), but less abundant diatom taxa include *Fragilariopsis curta* (6–45%), resting spores of *Hyalochaete Chaetoceros* spp. (9–50%) and vegetative valves of *Chaetoceros* spp. (*Hyalochaete*: <9%, subgenus *Phaeoceros*: <3%). The excellent preservation of *C. pennatum* and the relatively low content of terrigenous particles, including ice-rafted debris (IRD), suggest rapid deposition under open-water conditions. In general, the diatom species assemblage in Unit II of core VC424, in particular between 270 and 230 cm below seafloor (cmbsf), resembles that of the other cores, but the abundance of *C. pennatum* is ~10% lower. Moreover, the diatom assemblages occurring in the diatomaceous ooze and diatomaceous mud layers at site VC424 also include higher numbers of the species *Chaetoceros dichaeta* (<8%), *Proboscia inermis* (<35%) and *Pseudo-nitzschia lineola* (<15%), which are very rare to absent at the other sites. Additionally, Unit II of core VC424 is characterised by high abundances of *Chaetoceros* resting spores (24–76%), which are less frequent in Unit II of cores PS69/273-2, PS69/274-1, PS69/275-1 and VC425. As such the diatom assemblage in Unit II of core VC424 points to deposition in a similar, but more distal glaciomarine environment characterised by even longer open-water seasons.

Unit II is underlain by grey to olive, 42–125 cm thick terrigenous muddy to sandy sediments (Unit III). The uppermost section of Unit III (Unit IIIa) is mainly bioturbated, and exhibits SS values similar to those in Unit I and MS values slightly higher than in Unit I (Fig. 2). The biogenic opal content in Unit IIIa of core PS69/274-1 is 1–4 wt%, and the TOC content is 0.2–0.3 wt% (Fig. 2). Diatom concentrations in Unit IIIa of this core are $\leq 47 \times 10^6$ valves g^{-1}, but generally lower than in Unit I. The lower section of Unit III (Unit IIIb) is barren of diatoms and contains $\leq$2 wt% biogenic opal and $\leq$0.2 wt% TOC (Fig. 2). Unit IIIb comprises strongly laminated to stratified sorted sands and muds. It exhibits MS values up to $300–550 \times 10^{-5}$ SI units and SS values up to 9 kPa in the gravity cores, and MS values up to $90–280 \times 10^{-5}$ SI units and SS values up to 3 kPa in the vibrocores (Fig. 2). Coarse components comprising sand, gravel and pebbles increase down-core within Unit IIIb of core PS69/274-1 and in particular of core PS69/275-1, where intervals with normal grading occur. We conclude that Unit III was deposited in a proglacial setting under ice shelf or multi-year sea ice cover, in closer proximity to the grounding line of the West Antarctic Ice Sheet (WAIS) than Unit I. The general decrease of coarse-grained components towards the top of Unit III and the onset of bioturbation in Unit IIIa mirrors the increasing distance from the grounding line of the WAIS in response to its landward retreat.

Dark-grey to brownish-grey sandy and gravelly mud, sandy gravel, gravelly sand and diamictons (Unit IV) were recovered at the base of cores PS69/273-2, PS69/275-1, VC424 and VC425. MS values in Unit IV increase up to 750×10^{-5} SI units (maximum value in PS69/275-1 is around 1250×10^{-5} SI units) and SS values range from 4 to 13 kPa (Fig. 2). The diamictons are homogeneous to stratified, and lamination and normal grading characterise overlying and interbedded sandy to gravelly strata in cores PS69/275-1 and VC425. The sandy–gravelly sediments and the diamictons, at least in the upper section of Unit IV, are likely to represent a mixture of turbidites, debris flows, rain-out debris and meltwater-derived sediments that were deposited in a sub-ice shelf environment directly at the grounding line of the retreating WAIS (cf. Anderson, 1999; Domack *et al.*, 1999a; Licht *et al.*, 1999; Evans and Pudsey, 2002; Hillenbrand *et al.*, 2005). The basal diamicton in the lower section of Unit IV, in particular at site PS69/275-1, was possibly deposited as a soft till at the base of an expanded WAIS during the LGM (cf. Anderson, 1999; Domack *et al.*, 1999a; Licht *et al.*, 1999; Evans and Pudsey, 2002; Hillenbrand *et al.*, 2005).

DOI: 10.1002/jqs

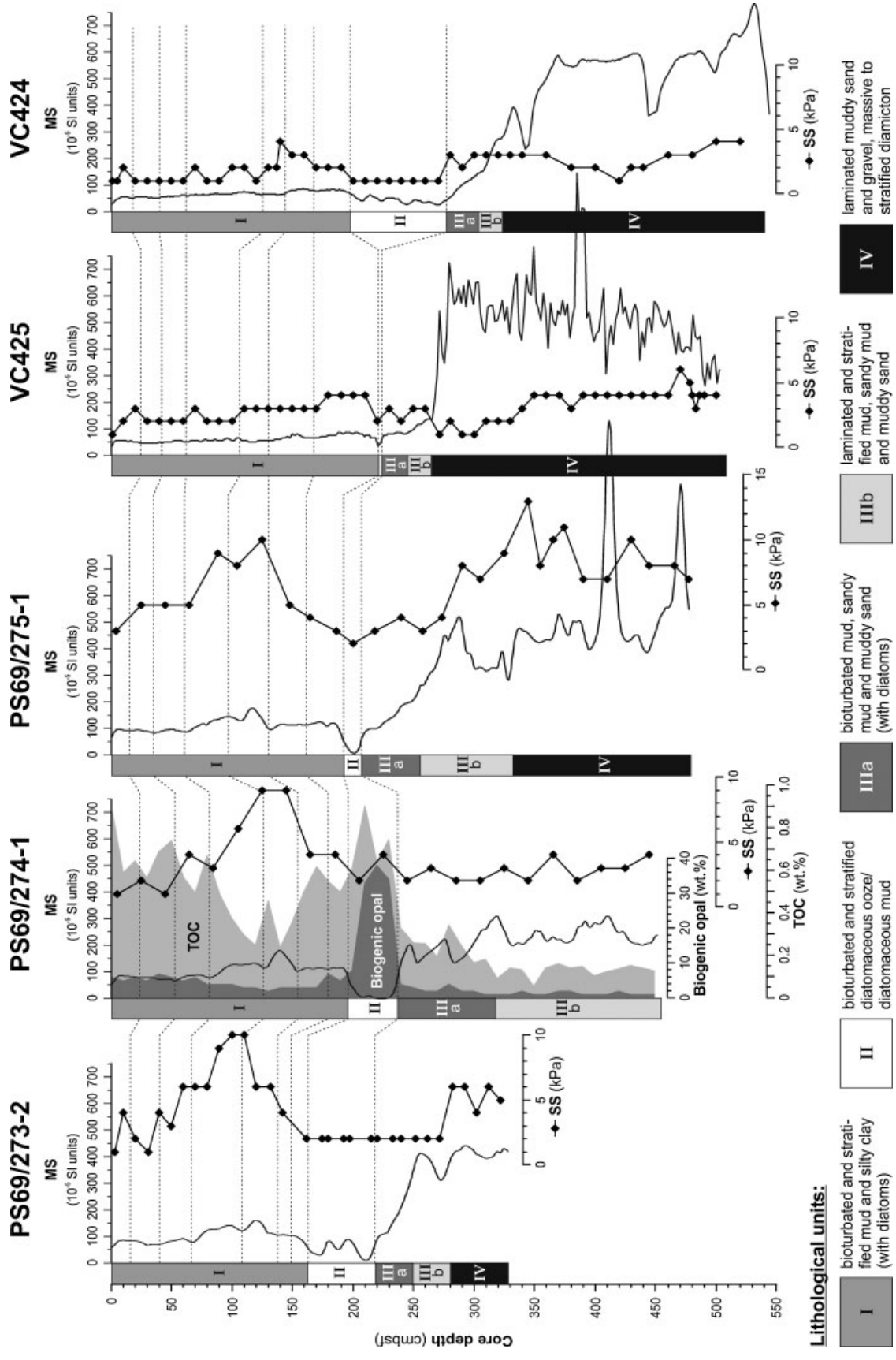

Figure 2 Lithological units (Unit I to Unit IV, for detailed explanation see main text) and physical properties (MS, magnetic susceptibility; SS, shear strength, marked by diamonds) of the studied cores. MS profile displayed for core VC425 was measured with a Bartington MS2F sensor, and MS profiles presented for all other cores were analysed with a MS2C sensor. Dotted lines indicate inter-core correlation on the basis of the MS down-core profiles (see Fig. 3). Contents of TOC (light grey shaded) and biogenic opal (dark grey shaded) are shown for core PS69/274-1 (note different scaling for biogenic opal and TOC)

DOI: 10.1002/jqs

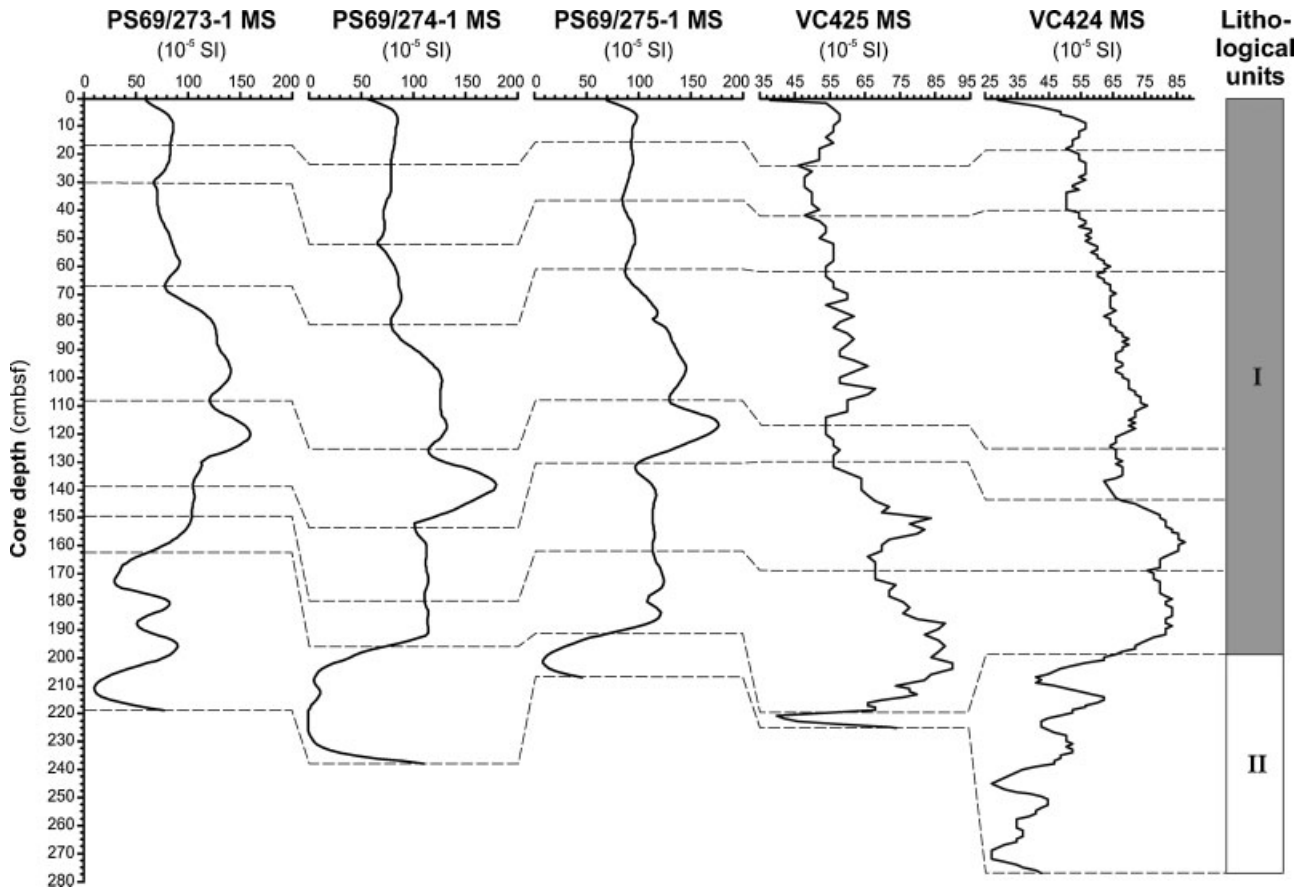

Figure 3 Correlation (hatched lines) of lithological Units I and II of the studied cores using their volume-specific magnetic susceptibility (MS) signal. MS profile displayed for core VC425 was measured with a Bartington MS2F sensor, and MS profiles presented for all other cores were analysed with a MS2C sensor. (Note: inter-core correlation was established by using all available MS and WBD data)

Excess ^{210}Pb activity

The excess ^{210}Pb activity at the surface of box core PS69/275-2 is 957 ± 108 Bq kg^{-1} and thus relatively high (Fig. 4). The excess ^{210}Pb profile reveals decay down to 7.5 cmbsf. A slight perturbation, probably caused by bioturbation, is observed between 3 and 4 cmbsf (Fig. 4). However, the depth interval affected by mixing is quite restricted, and the pertubation is not intense enough to mask the complete profile. The high activity of excess ^{210}Pb at the core surface combined with its down-core profile gives evidence that the core-top sediment of PS69/275-2 is unmodified by erosion, winnowing, condensation or mixing, and thus results from recent deposition (cf. Domack *et al.*, 2005; Pudsey *et al.*, 2006).

Radiocarbon chronology

The uncorrected AIO ages of the core tops in box cores PS69/275-2 and BC423, which also represent the tops of Unit I, are 3950 ± 35 and 4289 ± 35 ^{14}C a BP, respectively (Table 2). The excess ^{210}Pb data for core PS69/275-2 gives evidence for the recent deposition of the sediment surface, yielding an LCO of 2650 a for this site (assuming a 1300 a MRE). Similarly, we assume the core top at site BC423 results from modern sedimentation and infer an LCO of 2989 a (assuming a 1300 a MRE). Down-core conventional ^{14}C ages obtained from Unit I in cores PS69/274-1, PS69/275-1 and VC424 range from 7740 ± 39 to $14\,821 \pm 64$ ^{14}C a BP, corresponding to 4272–12 862 cal. a BP (Table 2).

The uncorrected AIO ages of bulk samples from Unit II are similar for all cores and vary from $11\,543 \pm 47$ ^{14}C a BP (PS69/275-1) to $13\,517 \pm 56$ ^{14}C a BP (VC424). The conventional ^{14}C ages of two bulk samples taken from the top and base of Unit II in core PS69/274-1 are $12\,034 \pm 69$ and $11\,967 \pm 49$ ^{14}C a BP, respectively (Table 2). Thus both dates are synchronous within analytical error and suggest rapid deposition of the diatom-rich unit. The AIO ages obtained from Unit II in core VC424 vary between $11\,803 \pm 48$ and $13\,517 \pm 56$ ^{14}C a BP and exhibit an age reversal. Subtraction of the LCO yields ages for Unit II that range from 8381 to 10 481 cal. a BP (both from VC424), which can be taken as minimum ages for its deposition. These minimum ages, however, result in age reversals in cores PS69/274-1 and PS69/275-1, if ages obtained from Unit I are taken into account. However, the relatively low terrigenous content of the diatomaceous ooze in Unit II suggests that we do not need to apply the full LCO for these samples since contamination from fossil carbon will be less significant (DeMaster *et al.*, 1996; Andrews *et al.*, 1999). Subtraction of only the MRE of 1300 a yields a range of calibrated dates from 11 956 cal. a BP (PS69/275-1) to 14 103 cal. a BP (VC424), which we consider as maximum ages for the deposition of Unit II (Table 2).

Replicate dating of the extracted AIO in acid-cleaned diatom hard parts from Unit II in core PS69/274-1 yielded uncorrected ages of 5106 ± 38 and 5111 ± 38 ^{14}C a BP, respectively (Table 2). We interpret these extraordinarily young ^{14}C dates as reflecting contamination by the adsorption of atmospheric CO_2 on the highly reactive opal surfaces of the extracted diatom hard parts prior to sample graphitisation and combustion for AMS ^{14}C dating (cf. Zheng *et al.*, 2002). It is also possible that

DOI: 10.1002/jqs

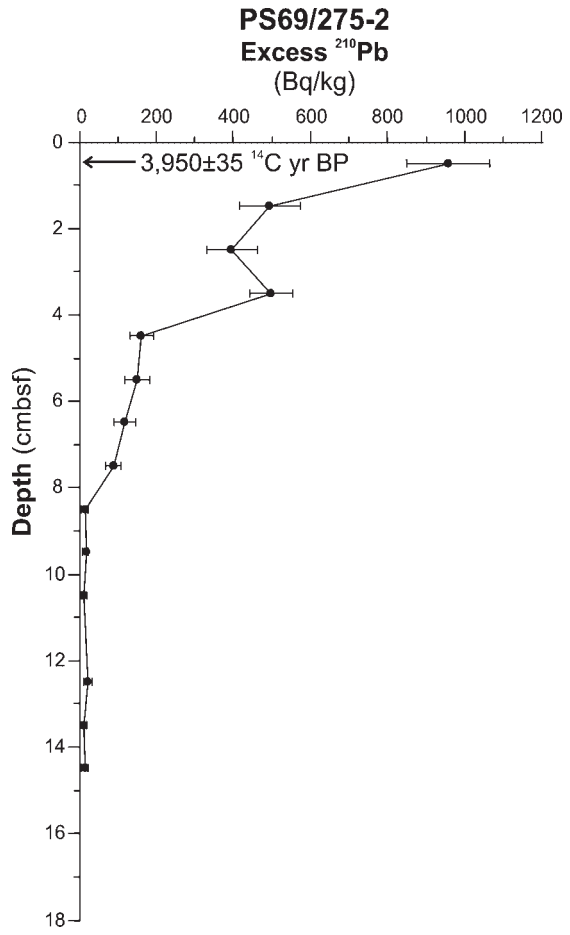

Figure 4 Down-core excess ^{210}Pb profile for giant box core PS69/275-2. The conventional ^{14}C age analysed on the AIO of the core-top sediment is also given

the AIO ^{14}C ages of the bulk samples from Unit II are affected by the incorporation of modern atmospheric CO_2, but obviously the CO_2 adsorption on extracted, acid-cleaned diatom hard parts is much more severe (Zheng *et al.*, 2002).

Conventional ^{14}C ages obtained from Unit IIIa in cores PS69/274-1 and PS69/275-1 are 24 416 ± 198 ^{14}C a BP (corresponding to 24 543 cal. a BP) and 15 703 ± 69 ^{14}C a BP (corresponding to 13 598 cal. a BP), respectively. An AIO sample dated from a muddy layer in Unit IV of core PS69/275-1 provided a relatively old age of 28 020 ± 311 ^{14}C a BP (Table 2).

Magnetic parameters and RPI

We measured magnetic parameters in cores VC424, PS69/274-1 and PS69/275-1 from the core top down into Unit III. The high concentration of coarse grains and the sedimentary texture both at the base of Unit IIIa and within Unit IIIb are likely to control magnetic properties and magnetic fabric in these samples (cf. Brachfeld *et al.*, 2003). Therefore, we only present and discuss the data from Units I, II and IIIa. The inclination of the NRM_{20mT} in Units I and IIIa varies around a mean value of ∼−80° (−83° ± 6° for VC424; −76° ± 9° for PS69/274-1; −81° ± 8° for PS69/275-1; Fig. 5(a)–(c)), which is close to (sub-)recent inclination values at our core sites according to the International Geomagnetic Reference Field IGRF-10 (−71° in AD 2009 and −76° in AD 1900). Anomalously shallow NRM_{20mT} inclinations (up to −53°) are observed at the core tops of VC424 and PS69/274-1. We interpret these anomalies as artefacts caused by the reorientation of magnetic particles during or after core recovery in response to the high water content of the surface sediments.

The ARM_{20mT} intensities, χlf values and ARM/κ ratios within Unit I of cores PS69/274-1 and PS69/275-1 range mainly from 120 to 280 mA m^{-1}, 40–70 × 10^{-8} m^3 kg^{-1} and 400–650 A m^{-1}, respectively (Fig. 5(a) and (b)). Exceptions are the intervals from 125 to 160 cmbsf in core PS69/274-1 and 105–130 cmbsf in core PS69/275-1, which are characterised by lower ARM_{20mT} intensities (down to 57 mA m^{-1}) and ARM/κ ratios (around 190–230 A m^{-1}) at their top and base, and slightly higher ARM_{20mT} intensities (up to 313 mA m^{-1}) in between. The ARM_{20mT} intensity within Unit I of core VC424 is generally lower (75–205 mA m^{-1}) than at the two gravity core sites, with χlf being remarkably constant (23–33 × 10^{-8} m^3 kg^{-1}) and the ARM/κ ratio varying from 380 to 930 A m^{-1} (Fig. 5(c)). In all three cores Unit II shows minima in ARM_{20mT} intensity and χlf, which can be attributed to the low concentration of terrigenous components and high water content in the diatom-rich sediments. Additionally, magnetite dissolution in the diatomaceous ooze may have occurred (Florindo *et al.*, 2003). The ARM/κ ratio also shows pronounced minima in Unit II of cores PS69/274-1 and PS69/275-1, indicating possible coarsening of the magnetic grain size (Fig. 5(a) and (b)). At all three sites the ARM_{20mT} intensities and the χlf values generally increase down-core within Unit IIIa (from 170 to 200 mA m^{-1} and 32 to 52 × 10^{-8} m^3 kg^{-1} in VC424; from 245 to 290 mA m^{-1} and 61 to 107 × 10^{-8} m^3 kg^{-1} in PS69/274-1; from 210 to 300 mA m^{-1} and 51 to 107 × 10^{-8} m^3 kg^{-1} in PS69/275-1). This coincides with a slight decrease in the ARM/κ ratios of Unit IIIa in cores PS69/275-1 and VC424 (Fig. 5(b) and (c)). The ARM_{20mT} intensities, χlf values and ARM/κ ratios from Unit I down to Unit IIIa vary within the same order of magnitude at all three core sites. This indicates that the studied sediments meet the magnetic uniformity criteria required for RPI investigations (cf. Brachfeld *et al.*, 2003; Macri *et al.*, 2006).

The RPI (NRM_{20mT}/ARM_{20mT}) values of cores PS69/274-1, PS69/275-1 and VC424 vary mainly between 0.10 and 0.40 (Fig. 5(a)–(c)). The RPI curves exhibit two broad maxima (with values >0.20 at sites PS69/274-1 and PS69/275-1, and values >0.15 at site VC424), one spanning the upper section of Unit I and the other spanning the lower section of Unit I, the whole of Unit II and the uppermost part of Unit IIIa. Anomalously low (<0.10) or high RPI values (>0.35 at sites PS69/274-1 and PS69/275-1, >0.30 at site VC424), but supported by only one data point, occur near the top of core PS69/274-1, in the upper RPI maximum at site VC424, and in the centre of Unit II at sites PS69/274-1, PS69/275-1 and VC424 (Fig. 5(a)–(c)). We acknowledge that these and other 'anomalous' RPI values that are based on only one or two data points might be unreliable. However, even if these data points are ignored, we would still see a clear correlation between the RPI curves from the Amundsen Sea and the reference curves for global and regional palaeomagnetic intensity (Fig. 6).

Discussion

Chronology of postglacial sedimentation on the inner shelf of the western Amundsen Sea Embayment

The main results of the radiocarbon chronology can be summarised as follows: (i) the bulk AIO ^{14}C ages for Unit II are similar for all sites (12 535 ± 1039 ^{14}C a BP; Table 2), and (ii) age reversals occur in Units I and II of cores PS69/274-1, PS69/

DOI: 10.1002/jqs

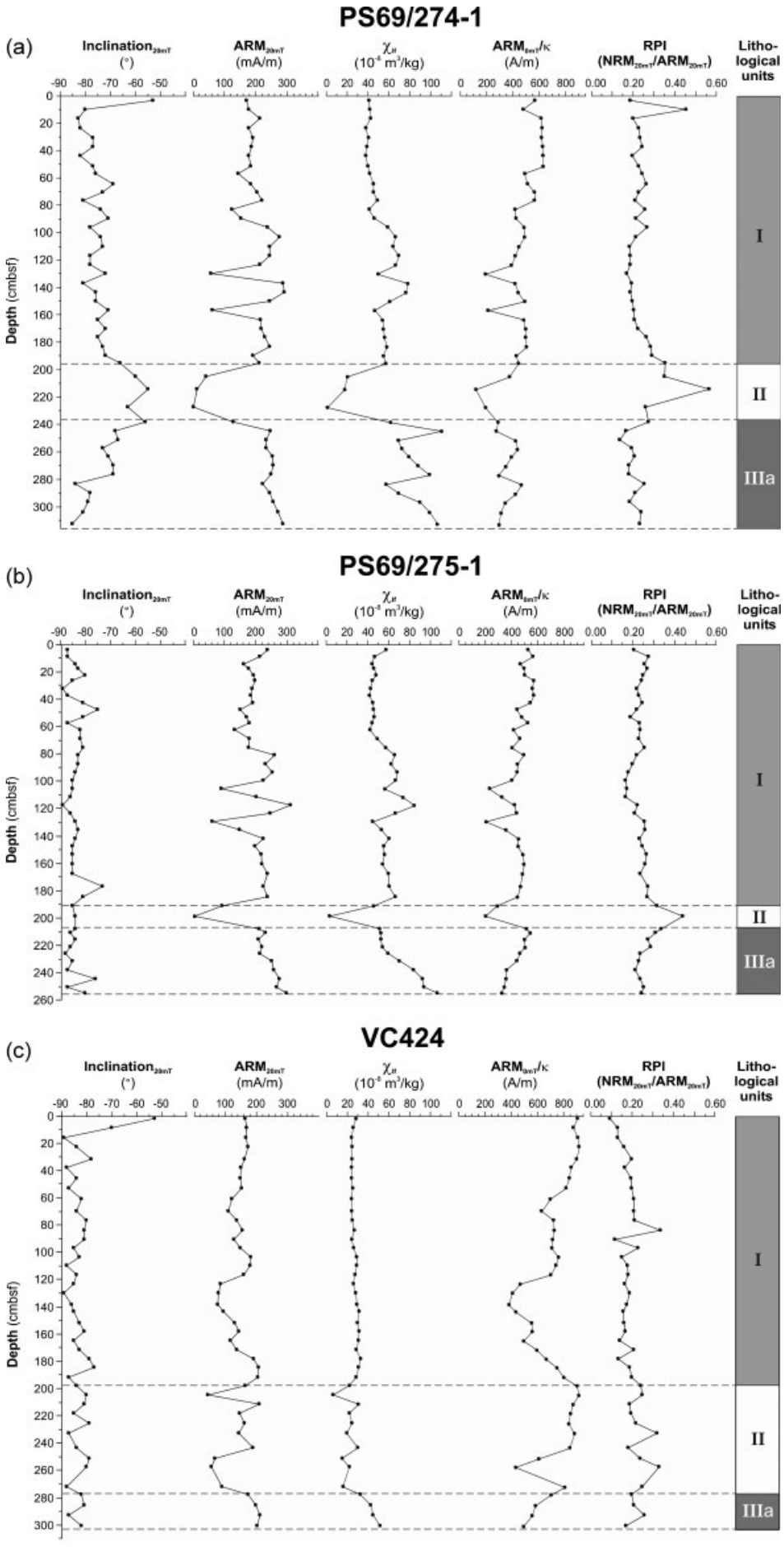

Figure 5 Inclination (at 20mT), ARM (at 20mT), mass-specific MS χlf, ARM/κ and RPI (NRM_{20mT}/ARM_{20mT}) for cores PS69/274-1 (a), PS69/275-1 (b) and VC424 (c). Lithological units are also given

DOI: 10.1002/jqs

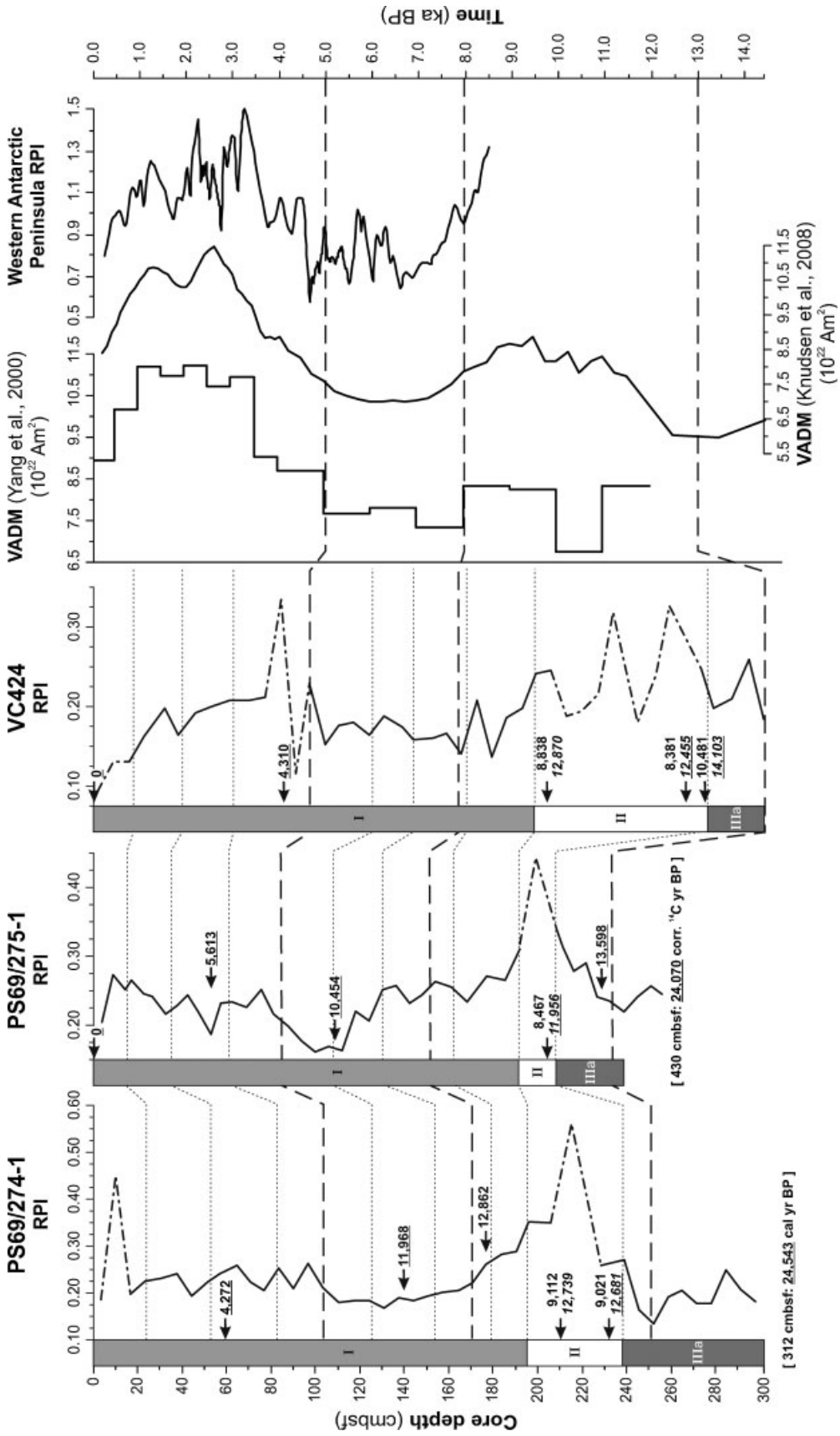

Figure 6 RPI of cores PS69/274-1, PS69/275-1 and VC424 in comparison with two global RPI reference curves (Yang *et al.*, 2000; Knudsen *et al.*, 2008) and a regional RPI reference curve from the shelf west of the Antarctic Peninsula (Willmott *et al.*, 2006). Lithological units are also shown (cf. Fig. 2). Dash-dotted lines indicate possibly unreliable RPI values, dotted lines indicate inter-core correlation on the basis of the MS profiles (cf. Fig. 3), and dashed lines indicate the correlation between the RPI records of the cores and the reference RPI curves. Bold numbers give calibrated AIO ^{14}C dates based on LCO and MRE correction, and numbers in italics give calibrated AIO ^{14}C dates based on MRE correction only (in cal. a BP). Dates used for the age models given in Table 3 are underscored

DOI: 10.1002/jqs

275-1 and VC424. After the LGM the MRE in the Southern Ocean (i.e. south of the APF) apparently varied by not more than 700 a (Van Beek *et al.*, 2002). However, the age reversals between Units I and II in cores PS69/274-1 and PS69/275-1 are caused by discrepancies exceeding 1500 ^{14}C a, which implies that in the ASE also the LCO, and thus the contribution of reworked fossil carbon, must have changed significantly with time. Despite the age reversals, it is still possible to establish reasonable age models solely based on AIO ^{14}C dates for the cores by preferring (i) the younger ^{14}C date in case of an age reversal, and (ii) the maximum ^{14}C age obtained from the diatomaceous ooze (i.e. the ^{14}C dates that were corrected by only subtracting the MRE). The first approach is based on the fact that young AIO ^{14}C ages are apparently less affected by contamination with fossil carbon (see Introduction). The second approach is justified by the relatively low terrigenous content of the Unit II sediments, suggesting that their AIO ^{14}C dates are more likely to provide *true* ages (cf. Andrews *et al.*, 1999). The resulting age models for the cores (Table 3 and Fig. 6) indicate deposition of Unit II between 11 956 cal. a BP (PS69/275-1) and 13 420 cal. a BP (VC425).

In order to test the plausibility of these radiocarbon-based age models, we correlated the RPI records of the sediment cores with global and regional records of palaeomagnetic intensity, which provide independent age constraints (Fig. 6). The graphic correlation yields an age of ca. 5.0–0 ka for the upper RPI maximum in our cores, which is consistent with the calibrated ^{14}C ages obtained from the upper section of Unit I in cores PS69/274-1 and VC424, but inconsistent with the slightly older ^{14}C age of 5613 cal. a in core PS69/275-1. The broad RPI minimum that characterises the middle section of Unit I in our cores corresponds to a global and regional minimum in magnetic intensity from 8.0 to 5.0 ka. Thus the corresponding ^{14}C ages in cores PS69/274-1 and PS69/275-1 are apparently too old (Fig. 6) and likely to reflect a non-systematic change of the LCO.

Even though the global reference curve of Yang *et al.* (2000) and the regional RPI curve date back to only 12 ka and 8.5 ka, respectively, it seems that the lower RPI maximum in our cores should have an age of ca. 13.0–8.0 ka. This age constraint is consistent with most calibrated ^{14}C ages for Unit II, irrespective of the correction method (Tables 2 and 3 and Fig. 6). Only two calibrated ^{14}C ages of Unit II in cores VC424 and VC425 (which had been corrected by just subtracting the MRE) and the calibrated ^{14}C date obtained from the uppermost section of Unit IIIa in core PS69/275-1 are slightly too old (Fig. 6), which may have been caused by greater contamination with fossil carbon. The general agreement between the calibrated ^{14}C dates of Unit II and the age constraints based on the RPI correlations indicates that the AIO in the bulk samples taken from the diatomaceous ooze is largely unaffected by contamination with fossil terrigenous carbon or adsorption of modern atmospheric CO_2 prior to sample graphitisation and combustion for AMS ^{14}C dating (cf. Zheng *et al.*, 2002). Unit II in cores PS69/274-1, PS69/275-1 and VC424 is positioned in the middle of the lower RPI maximum, which suggests an age around 10.5 ka for the deposition of the diatom-rich unit. This date provides a minimum age for the retreat of grounded ice that had advanced across the shelf north of the Getz 'A' and Getz 'B' ice shelves during the LGM (e.g. Wellner *et al.*, 2001; Larter *et al.*, 2009; Smith *et al.*, 2009).

We consider the AIO ^{14}C ages obtained from Unit IIIa in core PS69/274-1 and from Unit IV in core PS69/275-1 (24 543 cal. a BP and 24 070 corrected ^{14}C a BP, respectively; Table 2) to be unreliable because of significant contamination with terrigenous fossil carbon. These sediments were deposited in a proglacial setting close to the grounding line, where the supply of reworked fossil carbon is very high (cf. Domack, 1992; Heroy and Anderson, 2007). Our conclusion is further supported by ^{14}C dates on calcareous material which indicate that the WAIS had retreated from the inner shelf directly to the west of our study area just before ca. 12 600 ± 100 corrected ^{14}C a BP (Anderson *et al.*, 2002).

Thus, the ^{14}C-based age models of cores PS69/274-1, PS69/275-1 and VC424 are consistent with the chronological constraints provided by the RPI correlations only for the upper part of Unit I and for Unit II. The corresponding sediments exhibit relatively high TOC contents (e.g. core PS69/274-1, Fig. 2). In agreement with previous studies in the western Ross Sea (Licht *et al.*, 1996; Andrews *et al.*, 1999; Domack *et al.*, 1999a; Licht and Andrews, 2002), we conclude that in the western ASE shelf sediments resulting from enhanced biological productivity provide the most reliable AIO ^{14}C dates. However, this finding contrasts with findings from the central Ross Sea shelf, where Licht and Andrews (2002) observed no significant relationship between the TOC contents and the ^{14}C ages of the sediments.

Table 3 Age models for cores PS69/274-1, PS69/275-1 and VC424 solely based on radiocarbon chronology. Uncalibrated ages (that were corrected for LCO and MRE) are highlighted in italics, and assumed ages are given in brackets

Core	Sample depth (cmbsf)	Lithology	Lithological unit	Conventional ^{14}C age (^{14}C a BP)	Age model (cal. a BP/ *corr. ^{14}C a BP*)
PS69/274-1	0	Mud	I	—	[0]
PS69/274-1	59.5–60.5	Mud	I	7 740 ± 39	4 272
PS69/274-1	139.5–140.5	Mud	I	14 199 ± 61	11 968
PS69/274-1	231.5–232.5	Diatomaceous ooze	II	11 967 ± 49	12 681
PS69/274-1	311.5–312.5	Mud	IIIa	24 416 ± 198	24 543
PS69/275-2/1	0	Mud	I	3 950 ± 35	*0*
PS69/275-1	52.5–53.5	Mud	I	8 795 ± 42	5 613
PS69/275-1	107.5–108.5	Mud	I	13 154 ± 56	10 454
PS69/275-1	203.5–204.5	Diatomaceous ooze	II	11 543 ± 47	11 956
PS69/275-1	228–229	Mud	IIIa	15 703 ± 69	13 598
PS69/275-1	429.5–430.5	Mud	IV	28 020 ± 311	*24 070*
BC423/VC424	0	Mud	I	4 289 ± 35	*0*
VC424	83.5–84.5	Mud	I	8 108 ± 40	4 310
VC424	265.5–266.5	Diatomaceous ooze	II	11 803 ± 48	12 455
VC424	275.5–276.5	Diatomaceous ooze	II	13 517 ± 56	14 103

DOI: 10.1002/jqs

Circum-Antarctic occurrence of postglacial diatomaceous oozes on the Antarctic shelf

Relatively pure diatomaceous oozes dominated by one particular diatom species or diatom genus with pristine preservation of the frustules were deposited elsewhere on the Antarctic continental shelf after the LGM (for locations see Fig. 7). Leventer *et al.* (1993) found a *Corethron pennatum* ooze layer in a sediment core recovered from Granite Harbor. This layer was deposited during the Medieval Warm Period at about 1 ka BP according to an age model based on corrected ^{14}C dates of the AIO (Leventer *et al.*, 1993). Brachfeld *et al.* (2003) described three diatomaceous ooze layers dominated by *Corethron pennatum* from postglacial sediments in a core recovered from the Larsen Shelf. Interestingly, the basal and top diatomaceous ooze layers have uncorrected AIO ages of 11 200 ± 100 and 11 000 ± 85 ^{14}C a BP, respectively, which are close to the ages obtained from the diatomaceous ooze in our cores (Table 2). However, Brachfeld *et al.* (2003) also dated the core from the Larsen Shelf using its RPI record, which yielded an age of only 3.8 ± 0.5 ka for the basal ooze layer and an age of 1.4 ± 0.25 ka for the top ooze layer. This huge age discrepancy probably results from the particularly high LCO on the Larsen Shelf caused by the substantial recycling of ancient organic matter from Mesozoic source rocks (Domack *et al.*, 2005; Pudsey *et al.*, 2006).

Frequent diatomaceous ooze layers dominated by *Corethron pennatum* and/or *Hyalochaete Chaetoceros* resting spores and *Chaetoceros* vegetative valves (both from *Hyalochaete Chaetoceros* and the *Phaeoceros* subgenus) occur in postglacial sediments deposited after 11 600 cal. a BP in Palmer Deep on the inner shelf west of the Antarctic Peninsula, with *Corethron*-dominated layers being particularly abundant from ca. 4400 to 1800 cal. a BP (Leventer *et al.*, 2002; Sjunneskog and Taylor, 2002; Taylor and Sjunneskog, 2002; Maddison *et al.*, 2005; radiocarbon chronology based on AIO and carbonate ages, see Domack *et al.*, 2001).

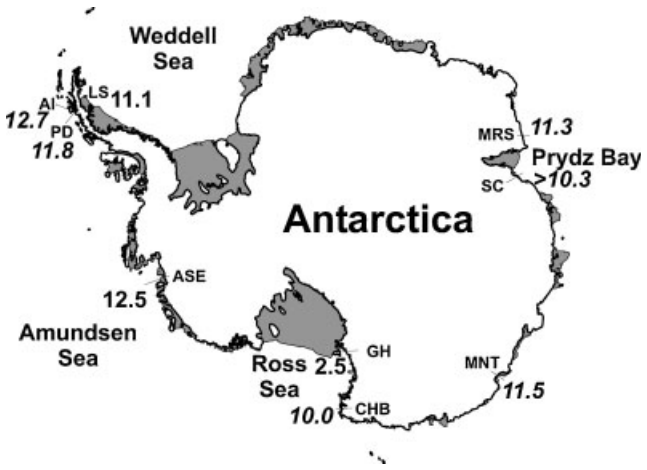

Figure 7 Occurrence and mean radiocarbon ages (in conventional ^{14}C a BP) of postglacial diatomaceous ooze layers deposited on the Antarctic shelf. Regular numbers give ages of layers dominated by *Corethron* spp. and numbers in italics give ages of layers dominated by resting spores of *Hyalochaete Chaetoceros* spp. Ice shelves are grey shaded. Locations and ^{14}C age references: AI, Anvers Island, Pudsey *et al.*, 1994; PD, Palmer Deep, Domack *et al.*, 2001; LS, Larsen Shelf, Brachfeld *et al.*, 2003; ASE, Amundsen Sea Embayment, this study; GH, Granite Harbor, Leventer *et al.*, 1993; CHB, Cape Hallett Bay, Finnochiaro *et al.*, 2005; MNT, Mertz-Ninnis Trough, Maddison *et al.*, 2006; SC, Svenner Channel, Leventer *et al.*, 2006; MRS, Mac.Robertson Shelf, Leventer *et al.*, 2006

Laminated diatomaceous ooze layers dominated by *Hyalochaete Chaetoceros* resting spores often characterise sediments that were deposited on the Antarctic shelf subsequent to grounded ice sheet retreat (Fig. 7). Such layers were reported from Palmer Deep between 12 250 ± 60 and 11 350 ± 75 ^{14}C a BP (corresponding to 13 180–11 460 cal. a BP; Sjunneskog and Taylor, 2002; Taylor and Sjunneskog, 2002; Maddison *et al.*, 2005; radiocarbon chronology based on AIO and carbonate ages, see Domack *et al.*, 2001), the western Antarctic Peninsula shelf near Anvers Island between 13 110 ± 120 and 12 280 ± 150 ^{14}C a BP (AIO ages; Pudsey *et al.*, 1994), the Mac.Robertson Shelf just to the west of Prydz Bay between 11 770 ± 45 (AIO age) and 10 870 ± 40 (carbonate age) ^{14}C a BP (corresponding to 11 450–10 710 cal. a BP; Stickley *et al.*, 2005; Leventer *et al.*, 2006), Svenner Channel in eastern Prydz Bay at some time between 26 960 ± 680 (AIO age) and 10 315 ± 50 (carbonate age) ^{14}C a BP (Leventer *et al.*, 2006), and Mertz-Ninnis Trough at some time between 10 400 ± 870 (carbonate age) and 7760 ± 50 (AIO age) ^{14}C a BP (Leventer *et al.*, 2006). Diatomaceous ooze laminae dominated by *Hyalochaete Chaetoceros* spp. resting spores, *Corethron pennatum*, *Rhizosolenia* spp. or mixed diatom species assemblages were reported from sediments deposited from 13 267 to 9809 ^{14}C a BP (uncorrected ages interpolated between AIO ages) in the Mertz-Ninnis Trough (Maddison *et al.*, 2006), while diatomaceous ooze laminae dominated by *Corethron pennatum*, *Hyalochaete Chaetoceros* resting spores and *Fragilariopsis curta* were deposited between 10 920 ± 50 and 9130 ± 40 (both AIO ages) ^{14}C a BP in Cape Hallett Bay in the western Ross Sea (Finocchiaro *et al.*, 2005).

Thus, *Chaetoceros*-rich laminae alternating with laminae characterised by a higher terrigenous content and mixed diatom assemblages were deposited on both the East Antarctic and the western Antarctic Peninsula shelf subsequent to grounded ice retreat. Leventer *et al.* (2006) attributed the rhythmically laminated sediments from the East Antarctic shelf to springtime blooms of *Chaetoceros* generated within well-stratified and restricted surface waters of calving bays that were influenced by the input of iron-rich meltwater. These authors attributed the interleaving, post-bloom summer/autumn laminae to downward flux of terrigenous material from melting glaciers and icebergs combined with the mixed diatom assemblages. Deposition of *Corethron*-rich ooze layers in Palmer Deep was associated with a well-stratified water column, generally warm climate conditions, an oceanographic event (such as convergence and sinking at a frontal boundary, which could further concentrate the frustules and enhance their rapid transport to and burial at the seafloor), and a joint occurrence of a large population of vegetative cells and a sexual reproductive event (Leventer *et al.*, 2002; Sjunneskog and Taylor, 2002; Taylor and Sjunneskog, 2002; Maddison *et al.*, 2005). In contrast to *Chaetoceros* blooms, however, the *Corethron* blooms probably occurred during summer time (Leventer *et al.*, 2002; Maddison *et al.*, 2005).

In the western ASE, the *Corethron*-rich diatomaceous ooze occurs directly above sediments deposited proximal to the grounding line. Additionally, the ^{14}C dates and the RPI correlations constrain its deposition to the time between 13.0 and 8.0 ka. These findings strongly suggest that the diatom-rich unit was deposited following deglaciation of the shelf, which took place before ca. 15 800 ± 3900 ^{14}C a BP in the eastern ASE and before ca. 13 873 ± 86 ^{14}C a BP directly to the west of the ASE (both carbonate ages; Anderson *et al.*, 2002). Similar to the deposition of the *Chaetoceros*- and the *Corethron*-dominated oozes in other sectors of the Antarctic shelf, we assume that well-stratified surface waters, relatively warm climatic conditions and oceanographic conditions

DOI: 10.1002/jqs

resulted in the rapid deposition and pristine preservation of the *Corethron*-rich ooze in the ASE.

The conventional ^{14}C chronology suggests that the deposition of the diatomaceous ooze in the western ASE may have coincided with the deposition of *Chaetoceros*- and *Corethron*-dominated ooze layers on the East Antarctic and Antarctic Peninsula shelf (Fig. 7). However, synchronous deposition of the diatomaceous ooze layers shown in Fig. 7 is difficult to explain, because ^{14}C ages on calcareous (micro-)fossils marking the onset of open-marine sedimentation after the LGM point to a time-transgressive deglaciation of the different sectors of the Antarctic shelf (Anderson *et al.*, 2002; Heroy and Anderson, 2005). Furthermore, Leventer *et al.* (2006) highlight the importance of local bathymetric and physiographic constraints for facilitating the deposition of pure diatomaceous ooze layers in calving bays on the East Antarctic shelf during the last deglaciation.

The RPI chronostratigraphy established by Brachfeld *et al.* (2003) for *Corethron*-rich ooze layers deposited on the Larsen Shelf clearly demonstrates that age assignments on the basis of AIO ^{14}C dates alone may be seriously flawed. Brachfeld *et al.* (2003) interpreted the *Corethron*-dominated ooze layers on the Larsen Shelf as indicators for the proximity to open-water productive events and consequently related them to mid to late Holocene ice shelf break-up in that area (e.g. Hodgson *et al.*, 2006). These findings indicate that the apparently synchronous deposition of relatively pure diatomaceous ooze layers at various sites of the Antarctic shelf as suggested by the radiocarbon chronology is rather coincidental. Physiography of the shelf and coast in conjunction with local to regional climatic warming and oceanographic processes associated with the break-up and melting of ice shelves, ice sheets and sea ice may be the most important factors for their deposition (Leventer *et al.*, 1993, 2002, 2006; Maddison *et al.*, 2005, 2006; Stickley *et al.*, 2005).

Conclusions

- The conventional AIO ^{14}C ages of undisturbed seafloor surface sediments collected from the inner shelf north of the eastern Getz Ice Shelf (western ASE) vary from 3950 ± 35 to 4289 ± 35 ^{14}C a BP. An excess ^{210}Pb activity profile measured at one of the sites demonstrates modern deposition and suggests that these old ^{14}C ages mainly arise from local contamination with fossil organic matter.
- Five sediment cores collected in the western ASE recovered a unit consisting of diatomaceous ooze and diatomaceous mud. The diatomaceous ooze is characterised by high concentrations of extremely well-preserved *Corethron pennatum* and was deposited following deglaciation of the shelf, probably in response to climatic and oceanographic conditions favouring rapid deposition and burial of the diatoms.
- The conventional AIO ^{14}C dates of bulk sediment samples taken from three of the cores reveal a few age reversals downcore, which are attributed to significant changes in local contamination with fossil organic matter through time.
- The AIO ^{14}C dates from the *Corethron*-rich ooze indicate its deposition between ca. 13 500 and 11 500 ^{14}C a BP. Depending on the correction method for these ^{14}C dates, their calibrated ages range from ca. 14 100 to 8400 cal. a BP. In contrast, the uncorrected AIO ^{14}C dates on diatom hard parts extracted from the diatomaceous ooze are only about 5100 ^{14}C a BP. We reject these ages as being too young due to the adsorption of modern atmospheric CO_2 onto the surface of the extracted diatom hard parts prior to sample graphitisation and combustion for AMS ^{14}C dating.
- The RPI records of three of the cores from the western ASE can be correlated with global and regional stacks of palaeomagnetic intensity. This correlation indicates that the sediments with the highest TOC contents provide more reliable AIO ^{14}C ages, and constrains the deposition of the diatom-rich sediments to the time between ca. 13.0 and 8.0 ka BP.
- The various age constraints for the deposition of the diatom-rich unit in the ASE suggest grounding-line retreat from the inner shelf before ca. 13.0 ka BP, which is consistent with previously obtained deglaciation ages for the region.
- According to the ^{14}C and RPI chronologies the deposition of the *Corethron*-rich ooze in the western ASE may have coincided with the deposition of diatomaceous ooze layers on both the East and West Antarctic shelf during the last deglaciation. However, the age constraints are still too unreliable to conclude a contemporaneous, circum-Antarctic event, and the apparent synchroneity may be no more than a coincidence.

Acknowledgements Our work was supported by the British Antarctic Survey (BAS) GRADES-QWAD and Palaeo-Ice Sheets projects, the Alfred Wegener Institute MARCOPOLI Programme and UK Natural Environment Research Council (NERC) New Investigator Grant NE/F000359/1. We are grateful to the captains, officers, crew, support staff and scientists who participated in cruises ANT-XXIII/4 and JR141, and acknowledge U. Bock, S. Wiebe, R. Froehlking and M. Seebeck (all AWI), who helped with core sampling and preparation. We thank S. Fitzer and J. Howe (both SAMS) for analysing the gamma samples and commenting on an earlier draft of the manuscript, respectively, and thank S. Brachfeld, K. Licht and an anonymous reviewer for their constructive reviews, which improved the manuscript.

References

Anderson JB. 1999. *Antarctic Marine Geology*. Cambridge University Press: Cambridge, UK.

Anderson JB, Shipp SS, Lowe AL, Wellner JS, Mosola AB. 2002. The Antarctic ice sheet during the last glacial maximum and its subsequent retreat history: a review. *Quaternary Science Reviews* **22**: 49–70.

Andrews JT, Domack EW, Cunningham WL, Leventer A, Licht KJ, Jull AJT, DeMaster DJ, Jennings AE. 1999. Problems and possible solutions concerning radiocarbon dating of surface marine sediments, Ross Sea, Antarctica. *Quaternary Research* **52**: 206–216.

Bentley MJ, Hodgson DA, Sugden DE, Roberts SJ, Smith JA, Leng MJ, Bryant C. 2005. Early Holocene retreat of the George VI Ice Shelf, Antarctic Peninsula. *Geology* **33**: 173–176.

Berkman PA, Forman SL. 1996. Pre-bomb radiocarbon and the reservoir correction for calcareous marine species in the Southern Ocean. *Geophysical Research Letters* **23**: 363–366.

Bianchi C, Gersonde R. 2004. Climate evolution at the last deglaciation: the role of the Southern Ocean. *Earth and Planetary Science Letters* **228**: 407–424.

Brachfeld S, Domack E, Kissel C, Laj C, Leventer A, Ishman S, Gilbert R, Camerlenghi A, Eglinton LB. 2003. Holocene history of the Larsen-A Ice Shelf constrained by geomagnetic paleointensity dating. *Geology* **31**: 749–752.

Conley DJ. 1998. An interlaboratory comparison for the measurement of biogenic silica in sediments. *Marine Chemistry* **63**: 39–48.

Crawford RM, Hinz F, Honeywill C. 1998. Three species of the diatom genus *Corethron castracane*: structure, distribution and taxonomy. *Diatom Research* **13**: 1–28.

DeMaster DJ, Ragueneau O, Nittrouer CA. 1996. Preservation efficiencies and accumulation rates for biogenic silica and organic C, N, and P in high-latitude sediments: the Ross Sea. *Journal of Geophysical Research C* **101**: 18501–18518.

DOI: 10.1002/jqs

Domack EW. 1992. Modern carbon-14 ages and reservoir corrections for the Antarctic Peninsula and Gerlache Strait area. *Antarctic Journal of the US* **27**: 63–64.

Domack EW, Jacobson EA, Shipp SS, Anderson JB. 1999a. Late Pleistocene/Holocene retreat of the West Antarctic Ice-Sheet system in the Ross Sea. Part 2: Sedimentological and stratigraphic signature. *Geological Society of America Bulletin* **111**: 1517–1536.

Domack EW, Taviani M, Rodriguez A. 1999b. Recent sediment remolding on a deep shelf, Ross Sea: implications for radiocarbon dating of Antarctic marine sediments. *Quaternary Science Reviews* **18**: 1445–1451.

Domack EW, Leventer A, Dunbar R, Taylor F, Brachfeld S, Sjunneskog C and ODP Leg 178 Scientific Party. 2001. Chronology of the Palmer Deep site, Antarctic Peninsula: a Holocene paleoenvironmental reference for the circum-Antarctic. *The Holocene* **11**: 1–9.

Domack E, Duran D, Leventer A, Ishman S, Doane S, McCallum S, Amblas D, Ring J, Gilbert R, Prentice M. 2005. Stability of the Larsen B ice shelf on the Antarctic Peninsula during the Holocene epoch. *Nature* **436**: 681–685.

Evans J, Pudsey CJ. 2002. Sedimentation associated with Antarctic Peninsula ice shelves: implications for paleoenvironmental reconstructions of glacimarine sediments. *Journal of the Geological Society (London)* **159**: 233–237.

Finocchiaro F, Langone L, Colizza E, Fontolan G, Giglio F, Tuzzi E. 2005. Record of the early Holocene warming in a laminated sediment core from Cape Hallett Bay (northern Victoria Land, Antarctica). *Global and Planetary Change* **45**: 193–206.

Florindo F, Roberts AP, Palmer MR. 2003. Magnetite dissolution in siliceous sediments. *Geochemistry, Geophysics Geosystems* **4**: 1053.

Forsberg CF, Løvlie R, Jansen E, Solheim A, Sejrup HP, Lie HE. 2003. A 1.3-Myr palaeoceanographic record from the continental margin off Dronning Maud Land, Antarctica. *Palaeogeography, Palaeoclimatology, Palaeoecology* **198**: 223–2235.

Geibert W, Rutgers van der Loeff MM, Usbeck R, Gersonde R, Kuhn G, Seeberg-Elverfeldt J. 2005. Quantifying the opal belt in the Atlantic and southeast Pacific sector of the Southern Ocean by means of ^{230}Th normalization. *Global Biogeochemical Cycles* **19**: GB4001.

Gersonde R, Zielinski U. 2000. The reconstruction of late Quaternary Antarctic sea-ice distribution: the use of diatoms as a proxy for sea-ice. *Palaeogeography, Palaeoclimatology, Palaeoecology* **162**: 263–286.

Gohl K. (ed.). 2007. The expedition ANTARKTIS-XXIII/4 of the Research Vessel 'Polarstern' in 2006. *Reports on Polar and Marine Research*, no. 557. Alfred Wegener Institute, Bremerhaven.

Goldstein SJ, Lea DW, Chakraborty S, Kashgarian M, Murrell MT. 2001. Uranium-series and radiocarbon geochronology of deep-sea corals: implications for Southern Ocean ventilation rates and the oceanic carbon cycle. *Earth and Planetary Science Letters* **193**: 167–182.

Gordon JE, Harkness DD. 1992. Magnitude and geographic variation of the radiocarbon content in Antarctic marine life: implications for reservoir corrections in radiocarbon dating. *Quaternary Science Reviews* **11**: 696–708.

Harden SL, DeMaster DJ, Nittrouer CA. 1992. Developing sediment geochronologies for high-latitude continental shelf deposits: a radiochemical approach. *Marine Geology* **103**: 69–97.

Heroy DC, Anderson JB. 2005. Ice-sheet extent of the Antarctic Peninsula region during the Last Glacial Maximum (LGM): insights from glacial geomorphology. *Geological Society of America Bulletin* **117**: 1497–1512.

Heroy DC, Anderson JB. 2007. Radiocarbon constraints on Antarctic Peninsula Ice Sheet retreat following the Last Glacial Maximum (LGM). *Quaternary Science Reviews* **26**: 3286–3297.

Hillenbrand C-D, Fütterer DK. 2002. Neogene to Quaternary deposition of opal on the continental rise west of the Antarctic Peninsula, ODP Leg 178, Sites 1095, 1096 and 1101. In *Proceedings of the Ocean Drilling Program Scientific Results*, Vol. 178, Barker PF, Camerlenghi A, Acton GD, Ramsay ATS (eds). Ocean Drilling Program, Texas A&M University: College Station, TX; 1–33 (CD-ROM).

Hillenbrand C-D, Baesler A, Grobe H. 2005. The sedimentary record of the last glaciation in the western Bellingshausen Sea (West Antarctica): implications for the interpretation of diamictons in a polar-marine setting. *Marine Geology* **216**: 191–204.

Hodgson DA, Bentley MJ, Roberts SJ, Smith JA, Sugden DE, Domack EW. 2006. Examining Holocene stability of Antarctic Peninsula ice shelves. *EOS* **87**: 305–312.

Howe JA, Shimmield TM, Diaz R. 2004. Deep-water sedimentary environments of the northwestern Weddell Sea and South Sandwich Islands, Antarctica. *Deep-Sea Research II* **51**: 1489–1514.

Hughen KA, Baillie MGL, Bard E, Beck JW, Bertrand CJH, Blackwell PG, Buck CE, Burr GS, Cutler KB, Damon PE, Edwards RL, Fairbanks RG, Friedrich M, Guilderson TP, Kromer B, McCormac G, Manning S, Ramsey CB, Reimer PJ, Reimer RW, Remmele S, Southon JR, Stuiver M, Talamo S, Taylor FW, van der Plicht J, Weyhenmeyer CE. 2004. Marine04 marine radiocarbon age calibration, 0–26 cal kyr BP. *Radiocarbon* **46**: 1059–1086.

Ingalls AE, Anderson RF, Pearson A. 2004. Radiocarbon dating of diatom-bound organic compounds. *Marine Chemistry* **92**: 91–105.

Knudsen MF, Riisager P, Donadini F, Snowball I, Muscheler R, Korhonen K, Pesonen LJ. 2008. Variations in the geomagnetic dipole moment during the Holocene and the past 50 kyr. *Earth and Planetary Science Letters* **272**: 319–329.

Laj C, Kissel C, Mazaud A, Michel E, Muscheler R, Beer J. 2002. Geomagnetic field intensity, North Atlantic Deep Water circulation and atmospheric Δ^{14}C during the last 50 kyr. *Earth and Planetary Science Letters* **200**: 177–190.

Larter RD, Gohl K, Hillenbrand C-D, Kuhn G, Deen TJ, Dietrich R, Eagles G, Johnson JS, Livermore R, Nitsche FO, Pudsey CJ, Schenke HW, Smith JA, Udintsev G, Uenzelmann-Neben G. 2007. West Antarctic Ice Sheet change since the last glacial period. *EOS* **88**: 189–191.

Larter RD, Graham AGC, Gohl K, Kuhn G, Hillenbrand C-D, Smith JA, Deen TJ, Livermore RA, Schenke HW. 2009. Subglacial bedforms reveal complex basal regime in a zone of paleo-ice stream convergence, Amundsen Sea Embayment, West Antarctica. *Geology* **37**: 411–414.

Leventer A, Dunbar R, DeMaster D. 1993. Diatom evidence for Late Holocene climatic events in Granite Harbor, Antarctica. *Paleoceanography* **8**: 373–386.

Leventer A, Domack EW, Barkoukis A, McAndrews B, Murray J. 2002. Laminations from the Palmer Deep: a diatom-based interpretation. *Paleoceanography* **17**: 8002.

Leventer A, Domack E, Dunbar R, Pike J, Stickley C, Maddison E, Brachfeld S, Manley P, McClennen C. 2006. Marine sediment record from the East Antarctic margin reveals dynamics of ice sheet recession. *GSA Today* **16**: 4–10.

Licht KJ, Andrews JT. 2002. The ^{14}C record of Late Pleistocene ice advance and retreat in the central Ross Sea, Antarctica. *Arctic, Antarctic and Alpine Research* **34**: 324–333.

Licht KJ, Jennings AE, Andrews JT, Williams KM. 1996. Chronology of late Wisconsin ice retreat from the western Ross Sea, Antarctica. *Geology* **24**: 223–226.

Licht KJ, Cunningham WL, Andrews JT, Domack EW, Jennings AE. 1998. Establishing chronologies from acid-insoluble organic ^{14}C dates on Antarctic (Ross Sea) and Arctic (North Atlantic) marine sediments. *Polar Research* **17**: 203–216.

Licht KJ, Dunbar NW, Andrews JT, Jennings AE. 1999. Distinguishing subglacial till and glacial marine diamictons in the western Ross Sea, Antarctica: implications for a Last Glacial Maximum grounding line. *Geological Society of America Bulletin* **111**: 91–103.

Macri P, Sagnotti L, Lucchi RG, Rebesco M. 2006. A stacked record of relative geomagnetic paleointensity for the past 270 kyr from the western continental rise of the Antarctic Peninsula. *Earth and Planetary Science Letters* **252**: 162–179.

Maddison E, Pike J, Leventer A, Domack E. 2005. Diatom rich sediments from Palmer Deep, Antarctica: seasonal and sub-seasonal record through the last deglaciation. *Journal of Quaternary Science* **20**: 435–446.

Maddison E, Pike J, Leventer A, Dunbar R, Brachfeld S, Domack E, Manley P, McClennen C. 2006. Post-glacial seasonal diatom record of the Mertz Glacial Polynya, East Antarctica. *Marine Micropaleontology* **60**: 66–88.

Maher BA. 1988. Magnetic properties of some synthetic sub-micron magnetites. *Geophysical Journal of the Royal Astronomical Society* **94**: 83–96.

DOI: 10.1002/jqs

Mosola AB, Anderson JB. 2006. Expansion and rapid retreat of the West Antarctic Ice Sheet in eastern Ross Sea: possible consequence of over-extended ice streams? *Quaternary Science Reviews* **25**: 2177–2196.

Müller PJ, Schneider R. 1993. An automated leaching method for the determination of opal in sediments and particulate matter. *Deep-Sea Research I* **40**: 425–444.

Nitsche FO, Jacobs SS, Larter RD, Gohl K. 2007. Bathymetry of the Amundsen Sea continental shelf: implications for geology, oceanography, and glaciology. *Geochemistry, Geophysics, Geosystems* **8**: Q10009.

Ó Cofaigh C, Dowdeswell JA, Allen CS, Hiemstra JF, Pudsey CJ, Evans J, Evans DJA. 2005. Flow dynamics and till genesis associated with a marine-based Antarctic palaeo-ice stream. *Quaternary Science Reviews* **24**: 709–740.

Ohkouchi N, Eglinton TI. 2006. Radiocarbon constraint on relict organic carbon contributions to Ross Sea sediments. *Geochemistry, Geophysics, Geosystems* **7**: Q04012.

Ohkouchi N, Eglinton TI. 2008. Compound-specific radiocarbon dating of Ross Sea sediments: a prospect for constructing chronologies in high-latitude oceanic sediments. *Quaternary Geochronology* **3**: 235–243.

Ohkouchi N, Eglinton TI, Hayes JM. 2003. Radiocarbon dating of individual fatty acids as a tool for refining Antarctic margin sediment chronologies. *Radiocarbon* **45**: 17–24.

Pudsey CJ. 2002. Neogene record of Antarctic Peninsula glaciation in continental rise sediments: ODP Leg 178, Site 1095. In *Proceedings of the Ocean Drilling Program Scientific Results*, Vol. 178, Barker PF, Camerlenghi A, Acton GD, Ramsay ATS (eds). Ocean Drilling Program, Texas A&M University, College Station, TX; 1–25 (CD-ROM).

Pudsey CJ, Barker PF, Larter RD. 1994. Ice sheet retreat from the Antarctic Peninsula shelf. *Continental Shelf Research* **14**: 1647–1675.

Pudsey CJ, Murray JW, Appleby P, Evans J. 2006. Ice shelf history from petrographic and foraminiferal evidence, Northeast Antarctic Peninsula. *Quaternary Science Reviews* **25**: 2357–2379.

Reimer PJ, Reimer RW. 2001. A marine reservoir correction database and on-line interface. *Radiocarbon* **43**: 461–463.

Rosenheim BE, Day MB, Domack E, Schrum H, Benthien A, Hays JM. 2008. Antarctic sediment chronology by programmed-temperature pyrolysis: methodology and data treatment. *Geochemistry, Geophysics, Geosystems* **9**: Q04005.

Sagnotti L, Macri P, Camerlenghi A, Rebesco M. 2001. Environmental magnetism of Antarctic late Pleistocene sediments and interhemispheric correlation of climatic events. *Earth and Planetary Science Letters* **192**: 65–80.

Schrader HJ, Gersonde R. 1978. Diatoms and silicoflagellates. In *Micropaleontological Counting Methods and Techniques: An Exercise on an Eight Metres Section of the Lower Pliocene of Capo Rossello, Sicily*, Zachariasse WJ *et al*. (eds). Micropaleontological Bulletin **17**: 129–176.

Siegert MJ, Barrett P, DeConto R, Dunbar R, Ó Cofaigh C, Passchier S, Naish T. 2008. Recent advances in understanding Antarctic climate evolution. *Antarctic Science* **20**: 313–325.

Sjunneskog C, Taylor F. 2002. Postglacial marine diatom record of the Palmer Deep, Antarctic Peninsula (ODP Leg 178, Site 1098) 1: Total diatom abundance. *Paleoceanography* **17**: PAL4.1–PAL4.8.

Smith JA, Hillenbrand C-D, Larter RD, Graham AGC, Kuhn G. 2009. The sediment infill of subglacial meltwater channels on the West Antarctic continental shelf. *Quaternary Research* **71**: 190–200.

St-Onge G, Stoner JS, Hillaire-Marcel C. 2003. Holocene paleomagnetic records from the St. Lawrence Estuary, eastern Canada: centennial- to millennial-scale geomagnetic modulation of cosmogenic isotopes. *Earth and Planetary Science Letters* **209**: 113–130.

Stickley CE, Pike J, Leventer J, Dunbar R, Domack EW, Brachfeld S, Manley P, McClennen C. 2005. Deglacial ocean and climate seasonality in laminated diatom sediments, Mac.Robertson Shelf, Antarctica. *Palaeogeography, Palaeoclimatology, Palaeoecology* **227**: 290–310.

Stuiver M, Reimer PJ, Reimer RW. 2005. CALIB 5.0 (http://calib.qub.ac.uk/calib/manual/).

Takada M, Tani A, Miura H, Moriwaki K, Nagatomo T. 2003. ESR dating of fossil shells in the Lützow-Holm Bay region, East Antarctica. *Quaternary Science Reviews* **22**: 1323–1328.

Taylor F, Sjunneskog C. 2002. Postglacial marine diatom record of the Palmer Deep, Antarctic Peninsula (ODP Leg 178, Site 1098) 2: Diatom assemblages. *Paleoceanography* **17**: PAL2.1–PAL2.12.

Theissen KM, Dunbar RB, Cooper AK, Mucciarone DA, Hoffmann D. 2003. The Pleistocene evolution of the East Antarctic Ice Sheet in the Prydz Bay region: stable isotopic evidence from ODP Site 1167. *Global and Planetary Change* **39**: 227–256.

Van Beek P, Reyss J-L, Paterne M, Gersonde R, Rutgers van der Loeff M, Kuhn G. 2002. ^{226}Ra in barite: absolute dating of Holocene Southern Ocean sediments and reconstruction of sea-surface reservoir ages. *Geology* **30**: 731–734.

Wellner JS, Lowe AL, Shipp SS, Anderson JB. 2001. Distribution of glacial geomorphic features on the Antarctic continental shelf and correlation with substrate: implications for ice behaviour. *Journal of Glaciology* **47**: 397–411.

Willmott V, Domack EW, Canals M, Brachfeld S. 2006. A high resolution relative paleointensity record from the Gerlache-Boyd paleo-ice stream region, northern Antarctic Peninsula. *Quaternary Research* **66**: 1–11.

Yang S, Odah H, Shaw J. 2000. Variations in the geomagnetic dipole moment over the last 12,000 years. *Geophysical Journal International* **140**: 158–162.

Zheng Y, Anderson RF, Froelich PN, Beck W, McNichol AP, Guilderson T. 2002. Challenges in radiocarbon dating organic carbon in opal-rich marine sediments. *Radiocarbon* **44**: 123–136.

Zielinski U, Gersonde R. 1997. Diatom distribution in Southern Ocean surface sediments (Atlantic sector): implications for paleoenvironmental reconstructions. *Palaeogeography, Palaeoclimatology, Palaeoecology* **129**: 213–250.

DOI: 10.1002/jqs